DOI:
10.1073/pnas.1714668115

Document Version
Peer reviewed version

Lipid bilayer composition modulates the unfolding free energy of a knotted alpha helical membrane protein

M.R. Sanders[1], H.E. Findlay[1] and P.J. Booth[1]

1: Department of Chemistry, Britannia house, King's College London Guy's Campus, 7 Trinity street, London, SE1 1DB, United Kingdom

Abstract

Alpha helical membrane proteins have eluded investigation of their thermodynamic stability in lipid bilayers. Reversible denaturation curves have enabled some headway in determining unfolding free energies. However, these parameters have been limited to detergent micelles or lipid bicelles, which do not possess the same mechanical properties as lipid bilayers that comprise the basis of natural membranes. We establish reversible unfolding of the membrane transporter LeuT in lipid bilayers, enabling the comparison of apparent unfolding free energies in different lipid compositions. LeuT is a bacterial orthologue of neurotransmitter transporters and contains a knot within its 12 transmembrane helical structure. Urea is used as a denaturant for LeuT in proteoliposomes, resulting in the loss of up to 30% helical structure depending upon the lipid bilayer composition. Urea unfolding of LeuT in liposomes is reversible, with refolding in the bilayer recovering the original helical structure and transport activity. A linear dependence of the unfolding free energy on urea concentration enables the free energy to be extrapolated to zero denaturant. Increasing lipid headgroup charge or chain lateral pressure increases the thermodynamic stability of LeuT. The mechanical and charge properties of the bilayer also affect the ability of urea to denature the protein. We thus gain insight not only to the long sought after thermodynamic stability of an alpha helical protein in a lipid bilayer, but also provide a basis for studies of the folding of knotted proteins in a membrane environment.

Significance Statement

Cells in our bodies sense and communicate with the outside world via proteins embedded in membranes that surround the cells. As with all proteins, a fundamental parameter governing their biological function is the inherent, thermodynamic stability of the folded state. Surprisingly there is no measure of this thermodynamic stability in a lipid membrane for the ubiquitous class of membrane proteins with structures based on alpha helices. We remedy this through the study of a protein related to the physiologically important membrane proteins that are partly responsible for

transmitting signals in the nervous system. We identify key properties of the surrounding lipid membrane that regulate the thermodynamic stability of the protein.

/body

Abbreviations: Sodium Dodecylsulphate (SDS), major facilitator superfamily (MFS), 1,2-dioleoyl-sn-glycero-3-phosphocholine (DOPC), 1,2-dioleoyl-*sn*-glycero-3-phosphoethanolamine (DOPE), 1,2-dielaidoyl-*sn*-glycero-3-phospho-(1'-*rac*-glycerol) (DOPG), neurotransmitter sodium symporter (NSS), Dodecyl maltopyranoside (DDM), Octyl-β-Glucoside (OG), BR (Bacteriorhodopsin), Diacyl glycerol Kinase (DGK)

Introduction

Knowledge of the energetics of protein reactions is necessary to generate physical descriptions of cellular processes. The thermodynamic stability of a protein is a fundamental parameter. A third of all cellular proteins reside in membranes and those with helical structures are ubiquitous across prokaryotes and eukaryotes. The hydrophobic character of these proteins together with their native membrane surroundings can make them experimentally challenging to study (1). As a result there is little information on key properties, including folding from their primary amino sequences to the final functional structure. Several lines of evidence suggest that these functional states of native integral membrane proteins are equilibrium structures (2). However, to date there are no thermodynamic measurements of the helical membrane protein class in lipid bilayers. The few thermodynamic stability measurements that exist for helical membrane proteins are in detergent micelles or bicelles, which do not adequately reproduce the properties of the lipid membrane that surrounds the proteins in cells. Evidence has emerged that charge and mechanical properties of the bilayer play an important role in the folding, stability and function of helical proteins (3). Such properties cannot be reproduced in micelles and only to a very limited extent in bicelles. Studies are therefore needed in lipid bilayers to determine the extent to which the fold of a membrane protein is dictated by the amino acid sequence and the surrounding lipid membrane. This not only advances membrane protein folding studies, by providing boundaries in which natural folding operates, but gives a physical basis for factors that alter membrane protein stability and misfolding linked to disease.

The hydrophobicity of membrane proteins means they have a high propensity to aggregate in aqueous solutions. In order to avoid aggregation, most helical proteins are thought to insert directly into the membrane co-translationally with the assistance of the translocon apparatus. Although the exact mechanism of membrane protein insertion is unclear, the final stages of protein folding are most likely to occur in the lipid bilayer (4, 5). Equally, lipids can induce post-translational re-positioning of helices and protein orientation within the membrane (6, 7). If the unique folded state is an equilibrium structure then it should be possible to achieve the folded structure via other pathways, as has been demonstrated for example from co-expression (8), re-assembly of protein fragments (9) or from cell-free synthesis (10). Moreover, it has proved possible to regain the folded structure of some membrane proteins from a partly denatured state in urea, by refolding directly into liposomes (11). Additionally, the stability of some membrane proteins is such that they can be successfully refolded in detergent micelles or mixed detergent/lipid mixtures (11-13). These latter systems have enabled insight into the thermodynamic stability of membrane proteins by translating the classical chemical denaturation approach of water-soluble proteins studies. A folded protein is denatured and a reversible refolding reaction established such that the free energy of unfolding can be determined between the folded and chemically unfolded state. The initial approach for helical membrane proteins used a partially denatured state in sodium dodecylsulfate (SDS) and established an equilibrium with a folded state in renaturing detergent micelles (14). The best studied case is bacteriorhodopsin for which folding rates and yields have been shown to be dependent on detergent, lipid dynamics, detergent/lipid concentrations and lipid bilayer mechanics (15-23). As a result, the unfolded state actually changes over time and thus is not at equilibrium. A comprehensive equilibrium and kinetic study overcame this and established a pseudo equilibrium over a specific time period, nonetheless extensive extrapolation to zero denaturant was required to attain a free energy of unfolding in the absence of SDS (24, 25). More recently a novel steric trapping approach was used, which employs different assumptions for equilibrium thermodynamic determination and avoids denaturants, instead using streptavidin binding to the doubly biotinylated protein and inducing partial unfolding (26). Urea has also proven useful in denaturing helical membrane proteins (11)and has moved the folding field forward to larger, more dynamic proteins; namely the 12 TM major facilitator superfamily (MFS) (12, 27). These proteins are partially denatured by urea and although the exact regions of the protein that are denatured are currently unknown, it seems likely that urea accesses aqueous exposed regions and those accessible via the substrate translocation site (11, 12, 27). Far UV circular dichroism provides a categorical measure of the partly denatured state in terms of secondary structure loss. To demonstrate correct refolding, we combine regain of function, coupled with recovery of helical structure.

Here we extend chemical denaturation approaches on membrane transporter proteins to free energy measurements in lipid bilayers. At present there have been no successful measurements of the thermodynamic stability of helical membrane proteins in bilayers. There have been thermodynamic studies of transmembrane helix oligomerisation in bilayers, using a variety of methods based on steric trapping (28), cross-linking (29), fluorescence resonance energy transfer (FRET) (30) and TOXCAT (based on Tox-R mediated activation of a chloramphenicol acetyltransferase gene) (31, 32). The equilibrium chemical denaturation approach we use here, enables us to probe the influence of the mechanical and charge properties of the lipid bilayer that are vital to the folding and function of membrane proteins (3). The charge across the membrane can be modified by head group alterations and is important for correct topology (33, 34). The lateral pressures within the bilayer that are imposed by lipids on the protein influence insertion (35, 36) and folding rates (37). These factors can be assessed in lipid bilayers and one way is to alter the lipid components. 1,2-dioleoyl-sn-glycero-3-phosphocholine (DOPC) lipids readily assemble to bilayers, however 1,2-dioleoyl-*sn*-glycero-3-phosphoethanolamine (DOPE) lipids themselves form non-bilayer phases. The introduction of PE into a bilayer PC reduces the pressure exerted laterally in the headgroup region but increases the outward chain lateral pressure. This has been shown to increase the activation energy of insertion of a helix across a bilayer and reduce folding yields (38). Introducing negatively charged 1,2-dioleoyl-*sn*-glycero-3-phospho-(1'-*rac*-glycerol) (DOPG) in PC bilayers also affects folding (39).

Our target protein is the prokaryotic sodium/leucine transporter LeuT, the first crystallographically resolved member of the neurotransmitter sodium symporter (NSS or SLC6) family (40, 41). In humans, NSS proteins are responsible for the re-uptake of neurotransmitters involved in synaptic transmission (42, 43). LeuT from *Aquifex aeolicus* comprises 12 transmembrane helices organised into two 5-helix inverted repeats with TMs 1-5 and 6-10 positioned on a pseudo two-fold axis, shown in figure 1 (44, 45). LeuT is an orthologue of Na^+ coupled neurotransmitter transporters in eukaryotes such as Dopamine active transporter (DAT) and the Serotonin transporter (SERT). Eukaryotic NSS proteins are physiologically important in humans, with NSS dysfunction being related to various chronic neurological disorders such as depression, epilepsy and Parkinson's disease (43).

Interestingly LeuT also contains a coupled figure-eight (4_1) trefoil (3_1) knot (46), shown in figure s1 (SI Appendix, figure S1). In recent years it has transpired that whilst knots are selected against in protein structures they are not completely avoided and account for 1 % of known structures in terms of PDB entries. Since membrane proteins remain underrepresented in the PDB, the extent of knotting in helical membrane proteins remains unknown. The complexity introduced by

entanglement in structures suggests natural knots may play a significant role. Computational and experimental studies of knotted proteins are currently focussed almost exclusively on a small number of water soluble proteins (47) and have led to postulations that knots may be important for activity or increasing protein stability. This first foray into the folding and stability of a knotted membrane protein, LeuT, thus provides key groundwork for further studies on how knots form at a molecular level in a membrane and why introducing such entanglements in membranes may be advantageous.

Here, we reconstitute LeuT into liposomes and use urea to denature the protein, monitoring the reduction in helical structure by far UV CD. The urea state is refolded by dilution into liposomes with the extent of refolding assessed by recovery of LeuT helical structure and transport activity. Reversible equilibria are established, leading to measurements of unfolding free energies at different urea concentrations. DOPE and DOPG are mixed with DOPC lipids to highlight possible effects of lateral pressure or head group charge on refolding.

Results

Reversible unfolding of LeuT in detergent Far UV CD spectroscopy showed purified, folded LeuT in 1 mM DDM to have 81 % α-helical secondary structure as shown in figure 2 (a), which concurs with the 76 % determined from the crystal structure in OG (48). Native mass spectrometry revealed LeuT to be monomeric, under our purification conditions, with the reproducible presence of bound phospholipids (~7-11 kDa) (SI Appendix, figure S2). Protein functionality was verified by reconstitution into liposomes and transport activity measured.

LeuT was reversibly unfolded by mixing purified protein in 1mM dodecyl-β-maltopyranoside (DDM) with urea, giving a final concentration of 8 M urea. In 8 M urea, far-UV CD showed a decrease in intensity of the negative 222 nm band from ~ 20,000 deg.cm^2.mol^{-1} to ~13,000 deg.cm^2.mol^{-1} indicating ~35 % reduction in LeuT α-helical structure (figure 2 (a) and table 1). The functionality of folded LeuT in detergent micelles was verified by transport assay after reconstitution into 0.5:0.5 DOPC:DOPG liposomes (figure 2 (b)). There was little to no transport activity when unfolded LeuT in 8 M urea was reconstituted into liposomes (figure 2 (b)). LeuT was refolded from 8 M Urea by dilution into 1 mM DDM micelles giving a final concentration of 0.8 M Urea. Refolding was illustrated by recovery of the original far-UV CD spectrum and the original LeuT substrate transport activity (see figures 2 (a) and (b)).

Urea equilibrium denaturation and refolding curves (see figure 2 (c)) were obtained as reported previously, using different samples for each urea concentration and repeating across different

protein preparations (11, 27). The folding and unfolding curves overlay, consistent with a reversible equilibrium folding reaction. The CD signal intensity at 222 nm was used as a measure of folded protein and the resulting values normalised between 0 and 100 %. Assuming the simplest model, the unfolding data were fit to a two state model between the urea-denatured state and the folded state, giving a free energy of unfolding at zero denaturant ΔG_u^{H2O} of +3.2 ± 0.3 kcal· mol^{-1} for LeuT in DDM micelles. Alternatively, unfolding free energies were also calculated at each urea concentration. A linear dependence of the free energy of unfolding on urea concentration was observed (figure 2 (d), giving an unfolding free energy at zero denaturant ΔG_u^{H2O} of +3.1 ± 0.3 kcal· mol^{-1}, consistent with the value obtained from direct fitting of the unfolding curve. It was not possible to determine free energy values below 2 M urea as LeuT remains largely folded at these low urea concentrations, thus it is possible the data in figure 2 (d) are not linear from 0-2 M urea.

Urea unfolding and refolding were also repeated on LeuT in 1 mM DDM in the presence of a second detergent, octyl glycoside (OG). Concentrations of OG up to 10 mM on the effect on the amount of structure lost during urea unfolding, the refolding efficiency or the resulting denaturation curve and thus ΔG_u^{H2O} (SI Appendix, figure s3).

LeuT reversibly unfolds at equilibrium within a lipid bilayer Purified LeuT in DDM was reconstituted into liposomes with a 0.8:0.2 mol ratio of DOPC:DOPE. Far UV CD showed that the secondary structure was retained, with 86 % α helical content as compared to 81 % in DDM (figure 3 (a)). These α helical contents are in agreement - as it is challenging to extract accurate values for samples in lipid bilayers due to various factors, including CD signal changes in the lipid environment and altered signal to noise as a result of lipid UV absorption (49). The functionality of reconstituted LeuT in liposomes was verified via the transport of ^{14}C leucine (figure 3 (b) (i)).

No denaturation of LeuT was observed when urea was added to the proteoliposomes (see SI Appendix, figure S5). We postulated that this was due to the inability of urea to access the protein or penetrate the lipid bilayer. Unfolding was therefore attempted in the presence of low concentrations of OG detergent, which may enable urea access to the protein since sub-solubilising amounts of OG will partition into the bilayer and alter the bilayer lateral pressure profile and permeabilisation (50). Several OG concentrations were tested (SI, Appendix, figure s6). A final concentration of 0.29 mM was chosen as it was the lowest OG concentration that enabled urea to denature LeuT in proteoliposomes. 0.29 mM OG is 86 fold lower than the critical micelle concentration, CMC) for OG of 25 mM. Previous work has shown that 40 mM OG (above the detergent CMC) reduces the binding efficiency of LeuT (41, 51).The addition of the very low, 0.29 mM OG concentration alone (in the absence of urea) had no effect on liposome size, homogeneity or

phase (with or without LeuT), as observed by dynamic light scattering (SI Appendix, figure s7) and ^{31}P NMR (SI Appendix, figure s8). The presence of 0.29 mM OG also had no observable effect on LeuT secondary structure, with LeuT in 0.8:0.2 DOPC:DOPE liposomes exhibiting native far UV CD (see figure3 (a) and (b)). Ion leakage across the bilayer was, however, observed with 0.29 mM OG, such that a sodium ion gradient could not be maintained to drive transport (SI Appendix, figure S9). The presence of a small amount of OG is therefore necessary to enable urea to denature the protein in the bilayers, but has no apparent effect on the protein structure, nor on the liposome size and phase. 0.29 mM OG was used in all liposomes experiments involving urea denaturation.

Far-UV CD showed a decrease in intensity of the negative 222 nm band when LeuT in 0.8:0.2 DOPC:DOPE liposomes was denatured by the addition of 8 M Urea in the presence of 0.29 mM OG. 35 % of the native helical content was lost, together with the ability of LeuT to transport substrate; similar to observed loss of helix and substrate transport after urea unfolding within DDM micelles (compare figures 2 (a) and (b) and 3 (a) and (b) (i)). Intrinsic tryptophan fluorescence measurements are also consistent with a significant loss of tertiary structure (SI Appendix, figure s10). LeuT was refolded by dilution of urea to a final concentration of 0.8 M urea, with OG diluted by a factor of 7000 to 0.04 nM. Successful refolding was indicated by the recovery of at least 95 % of the original helical structure, as determined by CD spectroscopy (see figure 3(a) (i)). Figure 3 (b) (i) shows that LeuT transport activity also recovered, as the very low 0.04 nM OG can maintain a sodium gradient. If a concentration of 0.29 mM OG (i.e. as used to enable urea unfolding) was kept constant during refolding, there was no discernible effect on the recovery of the original amount of helical structure, showing that refolding in terms of secondary structure is independent of OG concentration between 0.04 nM and 0.29 mM OG (SI Appendix, figure s11). However, the further dilution of OG to 0.04 nM enabled LeuT transport activity to be measured and thus was used in all refolding measurements.

Equilibrium unfolding measurements were made by incubating reconstituted LeuT in 0.29 mM OG in a range of urea concentrations, using CD intensity at 222 nm as a measure of folded protein. Equilibrium refolding was achieved by diluting the proteoliposomes at various urea concentrations. Figure 3 (c) shows that unfolding and refolding curves overlaid, consistent with reversible refolding at equilibrium. The OG concentration was constant at 0.04 nM for all refolding curves, and 0.29 mM for unfolding curves. These different concentrations of 0.29 mM and 0.04 nM OG thus had no effect on the agreement between the observed unfolding and refolding curves, respectively, and thus nor on the unfolding free energies determined from the curves. The free energy of unfolding at zero denaturant was determined by fitting the unfolding data in figure 3 (c) (i) to a two state folding model. Refolding data overlay and thus give the same free energy values (which, is independent of

OG concentration between 0.04 nM and 0.29 mM), but the unfolding data were used to determine the associated free energy change, as due to the higher protein concentrations attainable in these experiments, there are reduced errors. The free energies reported refer to recovery of a state with the original secondary structure and transport activity in the bilayer, as these properties are unaffected by the presence of 0.04 nM OG (6 x 10^{-5}- fold lower than the CMC). Unfolding data were collected at 0.5 M urea intervals with a minimum of four repeats. A linear free energy relationship was observed with urea concentration, enabling extrapolation to give the unfolded free energy in the absence of urea. This gave an overall free energy of unfolding at zero denaturant ΔG_u^{H2O} =+2.6 ± 0.1 kcal· mol^{-1}, for 0.8:0.2 DOPC:DOPE (see figure 3 (d) (i)). These values are slightly lower than the ΔG_u^{H2O} value obtained for LeuT in DDM of ΔG_u^{H2O} of +3.1 ± 0.3 kcal· mol^{-1}.

Reconstituted protein concentration had no effect on the denaturation or renaturation curves over a range of protein concentrations between 0.025-0.2 mg ml^{-1} in the bilayer; equivalent to 100:1-12.5:1 lipid to protein ratio by weight (SI Appendix, figure s12). This suggests that the higher protein concentrations, and the concentration used here of0.1 mg ml^{-1}, do not lead to aggregation in the bilayer. The fact that the unfolding and refolding curves overlay, without observable hysteresis, is also consistent with the absence of a protein concentration/aggregation affect.

Non bilayer lipid DOPE affects LeuT unfolding free energy The influence of the amount of the non-bilayer lipid DOPE present in the DOPC/DOPE bilayers on LeuT unfolding free energy was investigated as a means of altering lipid lateral pressure (52). Figure 3 (ii) shows data for reversible unfolding of LeuT in bilayers with increased DOPE content of 0.5 DOPC: 0.5 DOPE. Unfolding by 8M urea resulted in a reduction of ~30 % of the native helix content of LeuT, slightly less than the 35 % reduction observed at lower DOPE in 0.8:0.2 DOPE:DOPC (See figure 3 (a) (i) and table 1). The unfolding curve overlaid with the refolding curve and was fitted to a two state folding model (see figure 3 (c) (ii)). Extrapolation gave a free energy of unfolding at zero denaturant ΔG_u^{H2O} of +2.9 ± 0.2 kcal· mol^{-1} (see figure 3 (d) (ii)), which is a slightly larger free energy value than the ΔG_U^{H2O} of +2.6 ± 0.1 kcal· mol^{-1} at lower DOPE content in 0.8:0.2 DOPC:DOPE. Figure 5 shows that additional DOPE concentrations confirmed this trend of increasing ΔG_U^{H2O} with increasing DOPE content within DOPC:DOPE bilayers (see also SI Appendix, figure S13). The maximum DOPE mole fraction used was 0.5 to avoid the onset of non-bilayer phases that occur at higher DOPE concentrations.

Negatively charged DOPG affects LeuT unfolding free energy. The influence of headgroup charge on unfolding free energy of LeuT was investigated through the incorporation of increasing amounts of DOPG into DOPC liposomes. Folded LeuT in 0.8:0.2 DOPC:DOPG had the same secondary structure as that in DOPC:DOPE liposomes, as shown by far UV CD (figure 4 (b) (i), but a smaller reduction in helix

content was observed upon addition of 8 M urea. LeuT in 0.8:0.2 DOPC:DOPG lost ~20 % of total secondary structure upon urea denaturation (figure 4 (a) (i)); compared to 35 % in 0.8:0.2 DOPC:DOPE (see table 1). LeuT also exhibited reversible refolding in DOPC:DOPG liposomes, as shown by the recovery of secondary structure and transport activity in 0.8:0.2 DOPC:DOPG in figure 4 (a) (i) and (b) (i). The presence of differing amounts of PG appeared to influence the transport activity, nonetheless for each particular PG concentration; the transport activity of the original reconstituted protein was recovered upon refolding. Unfolding and refolding curves overlaid for LeuT in DOPC:DOPG, and a linear free energy relationship was observed with urea concentration(shown in figure 4 (c) (i). The extrapolated free energy of unfolding at zero denaturant for 0.8 PC: 0.2 PG, ΔG_u^{H2O} was +2.5± 0.1 kcal· mol^{-1} (see figure 4 (d) (i)). Figure 5 shows that increasing the DOPG content resulted in an increase in LeuT unfolding free energy, for example to give a ΔG_u^{H2O} of +3.8 ± 0.2 kcal· mol^{-1} at 0.5:0.5 DOPC/DOPG (see figures 4 (ii), SI appendix, figure S14 and table 1).

The influence of both non-bilayer and headgroup charged lipids on the stability of LeuT. LeuT reversible unfolding was also studied in a 1:1 DOPG:DOPE bilayer, without any DOPC present. Urea unfolding resulted in a small loss of 10 % of secondary structure, transport functionality was also lost upon unfolding. Unfolding and refolding data overlaid, but were linear with urea concentration as opposed to curved plots (see SI Appendix, figure s15). This could suggest increased stability of LeuT in a bilayer containing both DOPE and DOPG, but an unfolding free energy could not be determined.

Discussion

We have devised a fully reversible experimental system to study equilibrium folding of an α helical membrane protein in lipid bilayers. This has enabled the first determination of the thermodynamic stability of this class of protein in a bilayer. By extending classical chemical denaturation methods, the free energy of unfolding of LeuT has been measured from urea denaturation curves of the protein in a lipid bilayer. The linear dependence of the unfolding free energy on urea concentration allows extrapolation to zero denaturant and a free energy value in absence of urea. Membrane mechanical properties are known to modulate the folding, function and stability of integral membrane proteins (3). The only previous example directly linking thermodynamic stability of membranes proteins to lipid membrane forces are for a bacterial outer membrane protein with β–barrel structure (53-55). The unfolding free energy of LeuT is also dependent on lipid bilayer composition, indicating α-helical structure stability is also coupled to bilayer properties. The unfolding free energy of LeuT increases with increasing PE or PG in a PC bilayer, indicating that both

chain lateral pressure and negatively charged headgroups enhance the thermodynamic stability of LeuT, raising the magnitude of the unfolding free energy.

Urea has been shown to be a suitable denaturant of α helical membrane transporters, with reversible denaturant curves enabling free energies of unfolding to be determined for folded states in detergent micelles. This was demonstrated for members of the major facilitator superfamily (MFS); the galactoside transporters GalP and LacY from *E. coli* (11, 12). Additionally, urea can denature these proteins in lipid bilayers. However, although these MFS proteins can be refolded back into the bilayer it was not possible to establish reversible refolding to enable free energy measurements. It was recently demonstrated that the insertion, stability and functionality of LacY was heavily influenced by mechanical properties of the membrane (56); it is possible this effect could also carry over to reversibly unfolding in the membrane. MFS transporters have dynamic structures with 12 transmembrane helices (57, 58) arranged in 2 domains, whilst the 12 helices of LeuT are in a knotted arrangement (46). Urea seems to denature MFS proteins in part via the substrate binding site at the domain interface. It is however unknown how much of the membrane embedded regions are effected by urea and therefore the nature of the unfolding transition is unclear. In contrast, folding and stability of knotted membrane proteins has not been studied. The results here show that LeuT is more stable than the MFS proteins, and there is no loss of secondary structure upon addition of urea to LeuT in lipid bilayers (shown in S5 (a)). To enable urea to denature LeuT a small amount of detergent OG is added to the bilayers; almost 100-fold lower than the CMC and 10-fold less than that used to pre-saturate liposomes during reconstitution. The addition of this small amount of OG detergent does not affect the structure or phase of the liposomes as seen by ^{31}P NMR and DLS, nor does it alter the protein structure. The OG nonetheless will partition into the bilayer, enabling urea to induce denaturation of LeuT; it is possible that OG affects the lateral packing pressure of the surrounding bilayer, similarly to an earlier report (50). The successfully refolded state and agreement of the unfolding and refolding curves are independent of OG.

The urea-denatured states of MFS and LeuT proteins are partly structured. 8 M urea induces ~ 30 % reduction in α helical structure for GalP and LacY MFS proteins, whilst LeuT loses ~35 % helicity upon 8 M urea denaturation in DDM micelles or ~30 % helicity in DOPC/DOPE (4:1 mole ratio) in the presence of 0.29 mM OG. The ability of urea to denature LeuT is dependent upon the lipid composition. Increasing lipid chain lateral pressure and headgroup charge increases the stability of LeuT to 8 M urea. A smaller reduction in helix is seen upon 8 M urea addition to DOPC liposomes with increasing amounts of DOPE or DOPG (table 1). LeuT suffers only a 10 % reduction in helical

structure in charged liposomes containing both DOPE and DOPG lipids upon the addition of 8 M urea. LeuT was functional in all liposomes studied, but lost transport activity when urea was added and regained > 90 % transport activity and original secondary structure content upon refolding in the liposomes (0.8 M Urea, 0.04 nM OG), indicating refolding is highly efficient.

The free energy for unfolding of LeuT in DDM, extrapolated to zero urea denaturant, ΔG_U^{H2O}, is found to be +3.1 ± 0.26 kcal· mol^{-1}. This is higher than the ΔG_U^{H2O} determined in DDM for GalP and LacY, which are both ~ +2.5 kcal.mol^{-1}. The free energy of unfolding of LeuT when reconstituted into DOPC/DOPE (4:1 mole ratio) ΔG_U^{H2O} is found to be +2.55 ± 0.14 kcal· mol^{-1}, which is lower than ΔG_U^{H2O} of LeuT in detergent micelles. This ΔG_U^{H2O} for LeuT increases to +2.94 ± 0.22 kcal· mol^{-1} in DOPC/DOPE (1:1 mole ratio) when the concentration of DOPE, and chain lateral pressure, is increased (see figure 5). A further increase is observed if charge is introduced to DOPC bilayers, with ΔG_U^{H2O} being +3.8 ± 0.23 kcal.mol^{-1} in DOPC/DOPG bilayers (1:1 mole ratio).

The ΔG_U^{H2O} free energy values quoted are for unfolding in lipid bilayers with no urea present, and for the unfolding reaction between the folded state and the partly unfolded state. The only structural information for this latter unfolded state in urea is the secondary structure as determined from far UV CD. The unfolded states for DOPC/DOPE contain 70 % of the fully folded α helical content. LeuT is more resistant to unfolding in urea when within DOPC/DOPG bilayers, retaining 80 % of the folded α helical content in 8 M urea. In spite of the greater degree of structure present in the unfolded state in DOPC/DOPG bilayers, the free energy of unfolding of LeuT is greater in DOPC/DOPG than DOPC/DOPE. Thus headgroup charge plays a significant role in the thermodynamic stability of LeuT. The introduction of DOPE into DOPC bilayers results in little change in the unfolded state helicity but an increase in the unfolding free energy, showing that chain lateral pressure also influences LeuT stability. This is consistent with previous predictions that increased chain pressure would stabilise a helical bundle.

Fully denatured states of the α helical class of membrane proteins are rarely encountered *in vivo*, nor can fully denatured states be used in equilibrium refolding studies. Partly denatured states *in vitro* have allowed folding equilibria to be established and the determination of the associated free energy (59). Not all helical membrane proteins can be denatured by urea or harsh detergents such as SDS, and for those that are, only a few can be refolded from these partly denatured states. Key interactions and structure are therefore presumably present in the partly denatured states that can be successfully refolded into lipids, whilst the lack of refolding is very likely to reflect aggregation (60, 61). SDS was the first denaturant to be used for thermodynamic measurements of helical membrane proteins (14). As for urea-denatured states, the residual structure in the SDS-denatured

state of membrane proteins is not well understood. BR is the best characterised with respect to folding studies, with far UV CD indicating a significant reduction in helicity (22, 62) and DEER suggesting a smaller reduction in helix structure and more or less complete loss of helix, helix tertiary interactions (63). Less direct information is available for SDS denatured states of other proteins that have been the subject of unfolding studies, for example GlpG in SDS exhibits no loss of helical structure and very little change in fluorescence emission band, which in any case is challenging to assign to definitive structural change (10, 64, 65).

The use of urea denaturation in studies of membrane transporters gives a system with clear helical denaturation and ease of refolding by dilution directly into lipid bilayers. We find no evidence of urea (or OG at the concentrations well below the cmc here) affecting the lipid phase of liposomes by DLS or ^{31}P NMR. Moreover linear free energy relationships are observed for LeuT in bilayers with wide range of urea concentrations, as previously observed for MFS proteins in detergent (11, 12). The combined urea, OG (or mild detergent) approach to unfold the protein in the bilayer, as used here, could prove to be a starting point for future thermodynamic studies on other helical membrane proteins. However, since different proteins have different dependences on lipid bilayer properties the exact lipids, detergents and concentrations used are likely to need optimisation. The major advantage of the mixed urea/OG approach over solvent based approaches such as TFE, is that the membrane is kept intact enabling refolding in bilayers. Potential issues with SDS and TFE include the ability of both to induce α-helical structure in polypeptide chains (even where there are no native helices) as well as perturbing and solubilising the bilayer (66, 67).

The strong influence of the solubilising environment on the thermodynamic stability makes it difficult to compare absolute free energy of unfolding values for different membrane proteins. Nonetheless it is possible to make certain evaluations. As well as valid comparisons between the unfolding energies for LeuT in different lipid bilayers, this work enables a comparison of the unfolding free energy of LeuT in detergent micelles and lipid bilayers. There is little difference in free energy of the folded LeuT state in DDM compared to that in DOPC/DOPE bilayers, with reference to an unfolded state with 60-65 % native helical content. The stability of LeuT however is greater in DOPG/DOPE bilayers than DDM micelles. The surrounding solvent has a clear influence on membrane protein dynamics and stability and the precise nature of the underlying interactions in micelles as compared to bilayers are unknown. Therefore stabilising detergents are inherently used during membrane protein purification, but finding a lipid bilayer that provides optimal stability requires considerable manipulation of lipid composition (68). It has also previously been shown that

the transmembrane glycophorin dimer can be more stable in detergent micelles than lipid bilayers (28)

LeuT is native to the Archea *Aquifex aeolicus* where phosaphatidylcholine is rare (69) and therefore the lipid may not be as effective in stabilising the protein in the bilayer as the other compositions studied. Furthermore, it has to be taken into account that Archea membrane lipids are significantly more branched in the acyl region (70) than the synthetic phospholipids we have used, and such branching may play a role in determining stability of the protein in the bilayer. The thermodynamic comparisons here within PC/PE/PG bilayers show that charge and lateral pressure are important and can increase the thermodynamic stability of LeuT over that in micelles. In line with this charge role, the polar sugar headgroup of DDM may impart stability to LeuT giving it similar stability to that in a neutral bilayer. This provides further evidence indicating that direct comparisons between detergent, bilayer and other environments are not necessarily straightforward.

Figure 6 shows the ΔG_U^{H2O} values obtained here in bilayers compared to existing reports for membrane proteins in micelle and bicelles. There are only a small number of examples of thermodynamic stability measurements for membrane proteins (see table s2). The values are obtained under different experimental conditions and using different approaches and assumptions. The unfolding free energies determined for LeuT in lipid bilayers (ΔG_U^{H2O} ranging from +2.5 to +3.8 kcal.mol^{-1}) are of similar order of magnitude to that for LeuT in micelles as well as those previously reported for MFS proteins GalP and LacY in detergent micelles (11, 12). The values presented for the α helical multi domain transporters unfolded by urea are smaller than stability measurements made for some single domain helical membrane proteins in micelles or bicelles using SDS as denaturant. For cases where SDS has been shown to induce partial unfolding of helical structures (giving denatured states with ~65% or 80 % of native helix content for both bacteriorhodopsin and DGK), values of +20.6 kcal.mol^{-1} and +16 kcal.mol^{-1} have been reported for ΔG_U^{H2O} for bacteriorhodopsin (62) and trimeric diacylglycerolkinase (DGK), respectively (14). The long linear extrapolation may overestimate the +20.6 kcal.mol^{-1} bR unfolding free energy value, with steric trapping measurements reporting + 11 kcal.mol^{-1} (71). The unfolding states and folding reactions of bacteriorhodopsin are complex and there are various stages of binding of the retinal cofactor. SDS denaturation at equilibrium and steric trapping probably measure different folding reactions, with a dissimilar unfolded state sterically trapped by the streptavidin binding compared to that obtained via SDS denaturation (including with regard to retinal binding). Retinal binding could also account for an increased stability over other proteins; the free energy for non-covalent retinal binding (and associated protein folding) has been determined as -7 kcal.mol^{-1} (72) , and further stabilization is

thought to occur during covalent binding and final folding, for which an enthalpy change for of -95 kcal.mol^{-1} has been reported in membranes (73). There are also reports of unfolding free energies in detergent micelles using SDS as denaturant for DsbB and GlpG, with ΔG_U^{H2O} values of +4.4 kcal.mol^{-1} and +8.2 kcal.mol^{-1} (64, 74). In both these latter cases there is no reduction in helical structure in the SDS denatured state and little information on tertiary structure, hence the nature of the unfolding/folding reaction is less certain. Steric trapping provides a comparable unfolding free energy of + 8.4 kcal mol^{-1} for GlpG in detergent micelles (75), whilst a smaller value of ~ +4 kcal.mol^{-1}has been inferred from innovative mechanical unfolding studies (76) .

There are no other thermodynamic unfolding free energy measurements for helical membrane proteins in lipid bilayers. Values do exist for β barrel membrane proteins (53-55). β structured proteins are generally less hydrophobic, can often be fully denatured in urea and some have been reversibly refolded into bilayers giving the associated free energy of the unfolding reaction. β barrel proteins also have thermodynamic stabilities that are modulated by the bilayer properties (55). The native membrane of most of the barrel proteins studied is the outer membrane of *E. coli* which contains lipopolysaccharide primarily in a thinner outer bilayer leaflet and is enriched in PE in the inner leaflet (77). Studies of barrels have focussed on the non-native bilayer lipid, POPC, under varying conditions. A ΔG_U^{H2O} of +3.4 kcal.mol^{-1} was found for the β barrel protein OmpA, and the thermodynamic stability was also shown to increase with increasing PE content (55). Our results on LeuT show that an increase in chain lateral pressure, as caused by the introduction to PE to PC bilayer, increase the thermodynamic stability of both β barrel and α helical transmembrane structures. Table S2 and review (78) give other values obtained for β barrel proteins in bilayers under a variety of conditions.

In spite of significant advances, helical membrane proteins remain severely under-represented in protein folding studies. Experiments in bilayers are paramount to understand membrane protein folding. The advances reported here finally enable comparisons of thermodynamic stability in a bilayer. This has important ramifications. In addition to providing insight into the coupling of protein thermodynamic stability to bilayer mechanics and charge it will also enable comparison of the effect of mutations on unfolding free energies. In turn, combined with kinetic measurements, this has the potential to give information on folding intermediates and transition states in bilayers through ϕ value analyses (62). The LeuT fold contains a complex trefoil knot involving 55% of the total amino acids; 278 aa out of a total 511 aa in the protein from residue 15 to 293 encompassing the first 7 helices (shown in SI Appendix, figure s1 a) i)). LeuT unfolds reversibly losing up to 40 % of the secondary structure under both detergent and bilayer conditions. It is unclear how much of the knot

is perturbed by urea. Further work is required, for example using mutagenesis, in conjunction with the approach described here to identify how residues in different regions of the knot influence the free energy of LeuT.

Synthetic bilayer studies also provide information that cannot be gained in cellular membranes and are more informative comparison than detergent systems. Although this work moves helical membrane protein folding towards thermodynamic and mechanism in bilayers, the challenges must not be underestimated. The difficulties are illustrated in the time taken to reach this point where measurements can now begin in lipid bilayers. Folding studies commenced on helical membrane proteins in the late 1980's (79), followed a decade later by the establishment of chemical denaturation to probe thermodynamics in detergent (14, 80) and another decade later by the first phi value analyses to investigate transition states in bicelles (62). Yet another 9 years on, we report the ability to determine thermodynamic stability in lipid bilayers. This is however just the beginning of a new series of extensive experiments to translate the current state of the art micellar and bicellar folding approaches to lipid bilayers. Rather than focussing on a small model protein and in order that the results are more informative, we have deliberately ensured the system works for the knotted membrane protein LeuT, a paralogue of human neurotransmitter transporters.

Methods and Materials

Methods

Protein expression and purification The expression and purification described here is a variation of that published by Singh et al (81). LeuT was expressed in One Shot BL21-AI Chemically competent *E.coli*. Cells were cultured in Terrific broth initially grown at 37 ^{O}C and induced for 20 hours at 20 ^{O}C. All buffers used in the purification contained 50mM Sodium phosphate (pH 7.4), 10 % (v/v) glycerol, 10 mM β-mercaptoethanol and 1mM DDM.

Equilibrium unfolding and refolding LeuT was unfolded and refolded in the detergent DDM using the method described in (11). The CD signal at 222 nm was used for further analysis and fitted as described in (11). For reversible LeuT unfolding in a bilayer, the protein was first reconstituted into one of the lipid compositions analysed (shown in table S1). Total lipid concentrations were kept at 10 mg ml^{-1} for all reconstitutions and mixed lipid compositions are given as mole fractions.~0.1 mgml^{-1} LeuT at a lipid to protein ratio of 25:1 was unfolded within the bilayer by a 1:5 dilution of 10 M Urea in the presence of 0.29 mM OG and 50 mM Sodium phosphate buffer (pH 7.4). Unfolding curves were constructed by mixing the protein in a range of Urea concentrations while keeping the OG

concentration constant. Refolding was carried out by fully unfolding the protein in 8 M urea and 0.29 mM OG and then diluting the proteoliposomes tenfold in buffer in a range of urea concentrations. The final OG concentration of 0.04 nM OG 75000 times less that the OG critical micelles concentration, with the lipid to OG mole ratio being 1000:1 and the protein to OG ratio being 180:1. Proteoliposomes were then concentrated down until the protein concentration was around 0.1 mg ml^{-1} in an Amicon spin concentrator blocked with Poly ethylene glycol, experimental conditions for all equilibrium folding experiments are shown in table S1. The unfolding curve was fitted to a two-state folding equation where the mean residue ellipticity in detergent or percentage secondary structure loss $\theta = \theta F - \theta U(\exp(m([\text{denaturant}] - Cm)/RT)/(1 + \exp(m([\text{denaturant}] - Cm)/RT)$. θF and θU are the CD values of the folded and unfolded states and Cm is the midpoint where there are equal amounts of folded and unfolded protein. The free energy of unfolding in the absence of denaturant is obtained from the fitted values, where $\Delta G_U^{H2O} = mCm$. The non-linear regression was carried out using GraFit software (Erithacus), and the standard error of the best-fit curve was calculated from the residuals.

Circular dichroism Spectroscopy All CD spectra were measured in an Aviv Circular Dichroism Spectrophotometer, Model 410 (Biomedical Inc., Lakewood, NJ, USA), with specially adapted sample detection to eliminate scattering artefacts, or at the Karlsruhe synchrotron (UV-CD12 beamline at ANKA, Karlsruhe Institute of Technology (82)). For reversible unfolding in detergent, the final protein concentration of 0.1–0.5 mg ml^{-1} was used in quartz rectangular or circular Suprasil demountable cells of pathlengths 0.1 mm, 0.2 mm or 0.5 mm (Hellma Analytics). Each sample was scanned two to four times from 260 to 190 nm. Samples containing urea were scanned from 260 to 200 nm due to the high absorbance of urea below 200 nm. The same cell containing buffer only was also measured for background subtraction during data analysis. All CD spectra were processed using CDTool (83), Dichroweb (84) and GraFit .

For reversible unfolding in liposomes, protein reconstitution was checked by scanning the proteoliposomes in circular Suprasil demountable, each sample was scanned four times from 260 to 190 nm, at 1-nm intervals with an averaging time of 3 s. The reconstituted protein was then unfolded and scanned in circular Suprasil demountable cells of pathlength 0.5 mm (Hellma Analytics). Samples containing urea were scanned from 260 to 210 nm due to the high absorbance of urea and the high scatter within samples containing liposomes.

Multiple scans were averaged and the buffer background was subtracted. These processed spectra were then imported in to GraFit for further analysis. The data was converted from mdeg to mean residue ellipticity, based upon protein concentration determined by UV absorbance at 280 nm or by

Markwell-Lowry protein concentration assay. The mean residue ellipticity at 222 nm was used for further analysis, by converting it into percentage of folded protein; where, 100% is fully folded protein and 0% is the amount of secondary structure remaining in 8 M urea. These percentages were then plotted against the urea concentration for comparison between fitting.

Transport assay Proteoliposomes were reconstituted as described in (85) by the detergent presaturation method (86) using LeuT suspended in gel filtration buffer. Reconstituted LeuT was unfolded and refolded using a scaled up version of procedure described above. L-Leucine uptake into liposomes was initiated by diluting liposomes loaded with buffer I (50 mM Potassium phosphate (pH 7.4), 250mM Potassium Chloride) with 20 fold excess of buffer II (50 mM Potassium phosphate (pH 7.4), 250mM Sodium Chloride, supplemented with 100 nM ^{14}C Leucine) at 25^{O}C. Transport of the reconstituted wild type protein was maintained for 15, 30, 45, 60, 75, 90, 120, 150, 180, 240, 300, 360 and 600 seconds, whereas for reconstituted LeuT that had undergone unfolding and refolding transport was maintained for 60, 120, 300 and 600 seconds, the transport was stopped by diluting each assay tenfold with ice cold buffer I. This was followed by filtration through 0.22 μM Nitrocellulose filters (Millipore, Watford, UK), the filters were then washed twice with 5 ml of ice cold buffer I. Filters were then placed in vials with ultima gold MV (Perkin Elmer) scintillation fluid and radioactivity was measured in a TRI-CARB 1600TR liquid scintillation counter.

Acknowledgements: We acknowledge funding from the European Research Council, ERC Advanced grant 294342 to PJ Booth as well as financial support from King's College, London. The authors would also like to thank E. Reading for help with native mass spectrometry as well as critically reading the manuscript, and R. Law for help with ^{31}P NMR data collection

References

1. Bowie JU (2005) Solving the membrane protein folding problem. *Nature* 438(7068):581-589.
2. Cymer F, von Heijne G, & White SH (2015) Mechanisms of Integral Membrane Protein Insertion and Folding. *Journal of Molecular Biology* 427(5):999-1022.
3. Booth PJ (2005) Sane in the membrane: designing systems to modulate membrane proteins. *Current Opinion in Structural Biology* 15(4):435-440.
4. Popot JL & Engelman DM (2000) Helical membrane protein folding, stability, and evolution. *Annual Review of Biochemistry* 69:881-922.
5. Engelman DM*, et al.* (2003) Membrane protein folding: beyond the two stage model. *FEBS Letters* 555(1):122-125.
6. Dowhan W & Bogdanov M (2011) Lipid-protein interactions as determinants of membrane protein structure and function. *Biochemical Society Transactions* 39:767-774.
7. Vitrac H, Bogdanov M, & Dowhan W (2013) In vitro reconstitution of lipid-dependent dual topology and postassembly topological switching of a membrane protein. *Proceedings of the National Academy of Sciences of the United States of America* 110(23):9338-9343.

8. Gorzelle BM*, et al.* (1999) Reconstitutive Refolding of Diacylglycerol Kinase, an Integral Membrane Protein. *Biochemistry* 38(49):16373-16382.
9. Di Bartolo ND, Hvorup RN, Locher KP, & Booth PJ (2011) In vitro folding and assembly of the Escherichia coli ATP-binding cassette transporter, BtuCD. *Journal of Biological Chemistry* 286(21):18807-18815.
10. Harris NJ*, et al.* (2017) Structure formation during translocon-unassisted co-translational membrane protein folding. *Scientific Reports* 7(1):8021.
11. Findlay HE, Rutherford NG, Henderson PJF, & Booth PJ (2010) Unfolding free energy of a two-domain transmembrane sugar transport protein. *Proceedings of the National Academy of Sciences of the United States of America* 107(43):18451-18456.
12. Harris NJ, Findlay HE, Simms J, Liu X, & Booth PJ (2014) Relative Domain Folding and Stability of a Membrane Transport Protein. *Journal of Molecular Biology* 426(8):1812-1825.
13. Tastan O, Dutta A, Booth P, & Klein-Seetharaman J (2014) Retinal proteins as model systems for membrane protein folding. *Biochimica Et Biophysica Acta-Bioenergetics* 1837(5):656-663.
14. Lau FW & Bowie JU (1997) A Method for Assessing the Stability of a Membrane Protein. *Biochemistry* 36(19):5884-5892.
15. Booth PJ (2005) Sane in the membrane: designing systems to modulate membrane proteins. *Curr. Opin. Struct. Biol.* 15:435-440.
16. Allen SJ, Curran AR, Templer RH, Meijberg W, & Booth PJ (2004) Controlling the folding efficiency of an integral membrane protein. *J. Mol. Biol.* 342:1293-1304.
17. Curran AR, Templer RH, & Booth PJ (1999) Modulation of folding and assembly of the membrane protein bacteriorhodopsin by intermolecular forces within the lipid bilayer. *Biochemistry* 38:9328-9336.
18. Booth PJ*, et al.* (1997) Evidence that bilayer bending rigidity affects membrane protein folding. *Biochemistry* 36:197-203.
19. Schlebach JP, Cao Z, Bowie JU, & Park C (2012) Revisiting the folding kinetics of bacteriorhodopsin. *Protein Sci* 21(1):97-106.
20. Braiman MS, Stern LJ, Chao BH, & Khorana HG (1987) Structure-function studies on bacteriorhodopsin. IV. Purification and renaturation of bacterio-opsin polypeptide expressed in Escherichia Coli. *J. Biol. Chem.* 262:9271-9276.
21. London E & Khorana HG (1982) Denaturation and renaturation of bacteriorhodopsin in detergents and lipid-detergent mixtures. *J. Biol. Chem.* 257:7003-7011.
22. Huang K-S, Bayley H, Liao M-J, London E, & Khorana HG (1981) Refolding of an integral membrane protein. Denaturation, renaturation and reconstitution of intact bacteriorhodopsin and two proteolytic fragments. *J. Biol. Chem.* 256:3802-3809.
23. Chen GQ & Gouaux E (1999) Probing the Folding and Unfolding of Wild-Type and Mutant Forms of Bacteriorhodopsin in Micellar Solutions: Evaluation of Reversible Unfolding Conditions. *Biochemistry* 38(46):15380-15387.
24. Curnow P & Booth PJ (2007) Combined kinetic and thermodynamic analysis of alpha-helical membrane protein unfolding. *Proceedings of the National Academy of Sciences of the United States of America* 104(48):18970-18975.
25. Curnow P & Booth PJ (2009) The transition state for integral membrane protein folding. *Proceedings of the National Academy of Sciences of the United States of America* 106(3):773-778.
26. Hong H, Blois TM, Cao Z, & Bowie JU (2010) Method to measure strong protein–protein interactions in lipid bilayers using a steric trap. *Proceedings of the National Academy of Sciences of the United States of America* 107(46):19802-19807.
27. Harris NJ*, et al.* (2017) Comparative stability of Major Facilitator Superfamily transport proteins. *European Biophysics Journal*:1-9.

28. Hong H & Bowie JU (2011) Dramatic Destabilization of Transmembrane Helix Interactions by Features of Natural Membrane Environments. *Journal of the American Chemical Society* 133(29):11389-11398.
29. Cristian L, Lear JD, & DeGrado WF (2003) Use of thiol-disulfide equilibria to measure the energetics of assembly of transmembrane helices in phospholipid bilayers. *Proceedings of the National Academy of Sciences of the United States of America* 100(25):14772-14777.
30. Chen L, Novicky L, Merzlyakov M, Hristov T, & Hristova K (2010) Measuring the Energetics of Membrane Protein Dimerization in Mammalian Membranes. *Journal of the American Chemical Society* 132(10):3628-3635.
31. Duong MT, Jaszewski TM, Fleming KG, & MacKenzie KR (2007) Changes in apparent free energy of helix-helix dimerization in a biological membrane due to point mutations. *J. Mol. Biol.* 371(2):422-434.
32. Russ WP & Engelman DM (1999) TOXCAT: A measure of transmembrane helix association in a biological membrane. *Proceedings of the National Academy of Sciences* 96(3):863-868.
33. Battle AR*, et al.* (2015) Lipid-protein interactions: Lessons learned from stress. *Biochimica Et Biophysica Acta-Biomembranes* 1848(9):1744-1756.
34. Platre MP & Jaillais Y (2017) Anionic lipids and the maintenance of membrane electrostatics in eukaryotes. *Plant Signaling & Behavior* 12(2).
35. Herrmann M, Danielczak B, Textor M, Klement J, & Keller S (2015) Modulating bilayer mechanical properties to promote the coupled folding and insertion of an integral membrane protein. *European Biophysics Journal with Biophysics Letters* 44(7):503-512.
36. Mirheydari M*, et al.* (2016) Insertion of perilipin 3 into a glycero(phospho)lipid monolayer depends on lipid headgroup and acyl chain species. *Journal of Lipid Research* 57(8):1465-1476.
37. Allen SJ, Curran AR, Templer RH, Meijberg W, & Booth PJ (2004) Controlling the folding efficiency of an integral membrane protein. *Journal of Molecular Biology* 342(4):1293-1304.
38. Lorch M & Booth PJ (2004) Insertion kinetics of a denatured alpha helical membrane protein into phospholipid bilayer vesicles. *Journal of Molecular Biology* 344(4):1109-1121.
39. Seddon AM*, et al.* (2008) Phosphatidylglycerol lipids enhance folding of an alpha helical membrane protein. *Journal of Molecular Biology* 380(3):548-556.
40. Shaffer PL, Goehring A, Shankaranarayanan A, & Gouaux E (2009) Structure and Mechanism of a Na+-Independent Amino Acid Transporter. *Science* 325(5943):1010-1014.
41. Quick M*, et al.* (2009) Binding of an octylglucoside detergent molecule in the second substrate (S2) site of LeuT establishes an inhibitor-bound conformation. *Proceedings of the National Academy of Sciences of the United States of America* 106(14):5563-5568.
42. Broer S & Gether U (2012) The solute carrier 6 family of transporters. *British Journal of Pharmacology* 167(2):256-278.
43. Pramod AB, Foster J, Carvelli L, & Henry LK (2013) SLC6 transporters: Structure, function, regulation, disease association and therapeutics. *Molecular Aspects of Medicine* 34(2-3):197-219.
44. Krishnamurthy H & Gouaux E (2012) X-ray structures of LeuT in substrate-free outward-open and apo inward-open states. *Nature* 481(7382):469-U480.
45. Yamashita A, Singh SK, Kawate T, Jin Y, & Gouaux E (2005) Crystal structure of a bacterial homologue of Na+/Cl--dependent neurotransmitter transporters. *Nature* 437(7056):215-223.
46. Jamroz M*, et al.* (2015) KnotProt: a database of proteins with knots and slipknots. *Nucleic Acids Research* 43(D1):D306-D314.
47. Niewieczerzal S & Sulkowska JI (2017) Knotting and unknotting proteins in the chaperonin cage: Effects of the excluded volume. *Plos One* 12(5).
48. Wang H, Elferich J, & Gouaux E (2012) Structures of LeuT in bicelles define conformation and substrate binding in a membrane-like context. *Nat Struct Mol Biol* 19(2):212-219.

49. Miles AJ & Wallace BA (2016) Circular dichroism spectroscopy of membrane proteins. *Chemical Society Reviews* 45(18):4859-4872.
50. Perozo E, Cortes DM, Sompornpisut P, Kloda A, & Martinac B (2002) Open channel structure of MscL and the gating mechanism of mechanosensitive channels. *Nature* 418:942.
51. Quick M, Shi L, Zehnpfennig B, Weinstein H, & Javitch J (2012) *Experimental conditions can obscure the second high-affinity site in LeuT* pp 207-211.
52. Gruner SM (1985) Intrinsic curvature hypothesis for biomembrane lipid composition: a role for nonbilayer lipids. *Proceedings of the National Academy of Sciences* 82(11):3665-3669.
53. Hong HD, Park S, Jimenez RHF, Rinehart D, & Tamm LK (2007) Role of aromatic side chains in the folding and thermodynamic stability of integral membrane proteins. *Journal of the American Chemical Society* 129(26):8320-8327.
54. Kleinschmidt JH & Tamm LK (2002) Secondary and tertiary structure formation of the beta-barrel membrane protein OmpA is synchronized and depends on membrane thickness. *J. Mol. Biol.* 324(2):319-330.
55. Tamm LK, Hong H, & Liang BY (2004) Folding and assembly of beta-barrel membrane proteins. *Biochimica Et Biophysica Acta-Biomembranes* 1666(1-2):250-263.
56. Findlay HE & Booth PJ (2017) The folding, stability and function of lactose permease differ in their dependence on bilayer lipid composition. *Scientific Reports* 7(1):13056.
57. Yan N (2013) Structural advances for the major facilitator superfamily (MFS) transporters. *Trends in Biochemical Sciences* 38(3):151-159.
58. Yan N (2015) Structural Biology of the Major Facilitator Superfamily Transporters. *Annual Review of Biophysics, Vol 44,* Annual Review of Biophysics, ed Dill KA), Vol 44, pp 257-283.
59. Booth PJ & Curnow P (2006) Membrane proteins shape up: understanding in vitro folding. *Current Opinion in Structural Biology* 16(4):480-488.
60. Di Bartolo N*, et al.* (2016) Complete Reversible Refolding of a G-Protein Coupled Receptor on a Solid Support. *PLOS ONE* 11(3):e0151582.
61. Lorch M & Booth PJ (2004) Insertion Kinetics of a Denatured α Helical Membrane Protein into Phospholipid Bilayer Vesicles. *Journal of Molecular Biology* 344(4):1109-1121.
62. Curnow P & Booth PJ (2007) Combined kinetic and thermodynamic analysis of α-helical membrane protein unfolding. *Proceedings of the National Academy of Sciences of the United States of America* 104(48):18970-18975.
63. Krishnamani V & Lanyi Janos K (2011) Structural Changes in Bacteriorhodopsin during In Vitro Refolding from a Partially Denatured State. *Biophysical Journal* 100(6):1559-1567.
64. Paslawski W*, et al.* (2015) Cooperative folding of a polytopic α-helical membrane protein involves a compact N-terminal nucleus and nonnative loops. *Proceedings of the National Academy of Sciences of the United States of America* 112(26):7978-7983.
65. Moon CP & Fleming KG (2011) Using tryptophan fluorescence to measure the stability of membrane proteins folded in liposomes. *Methods in enzymology* 492:189-211.
66. Barrera FN*, et al.* (2008) Protein Self-Assembly and Lipid Binding in the Folding of the Potassium Channel KcsA. *Biochemistry* 47(7):2123-2133.
67. Chill JH, Louis JM, Miller C, & Bax A (2006) NMR study of the tetrameric KcsA potassium channel in detergent micelles. *Protein Science : A Publication of the Protein Society* 15(4):684-698.
68. Columbus L (2015) Tuning Micelle Dimensions and Properties for Stabilizing Membrane Protein Fold and Function. *Biophysical Journal* 108(2):43A-43A.
69. Sohlenkamp C & Geiger O (2016) Bacterial membrane lipids: diversity in structures and pathways. *Fems Microbiology Reviews* 40(1):133-159.
70. Sturt HF, Summons RE, Smith K, Elvert M, & Hinrichs K-U (2004) Intact polar membrane lipids in prokaryotes and sediments deciphered by high-performance liquid chromatography/electrospray ionization multistage mass spectrometry—new biomarkers

for biogeochemistry and microbial ecology. *Rapid Communications in Mass Spectrometry* 18(6):617-628.
71. Chang Y-C & Bowie JU (2014) Measuring membrane protein stability under native conditions. *Proceedings of the National Academy of Sciences of the United States of America* 111(1):219-224.
72. Booth PJ, Farooq A, & Flitsch SL (1996) Retinal Binding during Folding and Assembly of the Membrane Protein Bacteriorhodopsin. *Biochemistry* 35(18):5902-5909.
73. Oesterhelt D, Meentzen M, & Schuhmann L (1973) Reversible Dissociation of the Purple Complex in Bacteriorhodopsin and Identification of 13-cis and all-trans-Retinal as its Chromophores. *European Journal of Biochemistry* 40(2):453-463.
74. Otzen DE (2003) Folding of DsbB in Mixed Micelles: A Kinetic Analysis of the Stability of a Bacterial Membrane Protein. *J. Mol. Biol.* 330(4):641-649.
75. Guo R*, et al.* (2016) Steric trapping reveals a cooperativity network in the intramembrane protease GlpG. *Nature chemical biology* 12(5):353-360.
76. Min D, Jefferson RE, Bowie JU, & Yoon T-Y (2015) Mapping the energy landscape for second-stage folding of a single membrane protein. *Nature chemical biology* 11(12):981-987.
77. Wu EL*, et al.* (2014) E. coli Outer Membrane and Interactions with OmpLA. *Biophysical Journal* 106(11):2493-2502.
78. Fleming KG (2014) Energetics of Membrane Protein Folding. *Annual Review of Biophysics* 43(1):233-255.
79. London E & Khorana HG (1982) DENATURATION AND RENATURATION OF BACTERIORHODOPSIN IN DETERGENTS AND LIPID-DETERGENT MIXTURES. *Journal of Biological Chemistry* 257(12):7003-7011.
80. Lau FW, Chen X, & Bowie JU (1999) Active Sites of Diacylglycerol Kinase from Escherichia coli Are Shared between Subunits. *Biochemistry* 38(17):5521-5527.
81. Singh SK, Piscitelli CL, Yamashita A, & Gouaux E (2008) A Competitive Inhibitor Traps LeuT in an Open-to-Out Conformation. *Science* 322(5908):1655-1661.
82. Bürck J*, et al.* (2015) UV-CD12: synchrotron radiation circular dichroism beamline at ANKA. *Journal of Synchrotron Radiation* 22(Pt 3):844-852.
83. Lees JG, Smith BR, Wien F, Miles AJ, & Wallace BA (2004) CDtool—an integrated software package for circular dichroism spectroscopic data processing, analysis, and archiving. *Analytical Biochemistry* 332(2):285-289.
84. Whitmore L & Wallace BA (2008) Protein secondary structure analyses from circular dichroism spectroscopy: Methods and reference databases. *Biopolymers* 89(5):392-400.
85. Putman M, Van Veen HW, Poolman B, & Konings WN (1999) Restrictive use of detergents in the functional reconstitution of the secondary multidrug transporter LmrP. *Biochemistry* 38(3):1002-1008.
86. Ollivon M, Lesieur S, Grabielle-Madelmont C, & Paternostre Mt (2000) Vesicle reconstitution from lipid–detergent mixed micelles. *Biochimica et Biophysica Acta (BBA) - Biomembranes* 1508(1–2):34-50.

Figure Legends

Figure 1: Crystal structure of LeuT in OG (PDBid:3GJD) taken from Quick et al (41). (a) Shows the full structure of the protein with the knot core highlighted in blue, the slipknot loop in yellow and the slipknot tail in green from opposite viewpoints taken from sequence data presented by knotprot database.

Figure 2: Unfolding and refolding of LeuT in 1 mM DDM detergent micelles by urea. (a) Far UV circular dichroism of LeuT in DDM (black), unfolded in 8 M Urea (red) and refolded into DDM (blue). (b) Transport of ^{14}C Leu into liposomes composed of 0.5:0.5 DOPC:DOPG by: initially folded LeuT (open circles) , LeuT unfolded and refolded followed by reconstitution into liposomes (blue squares). Control of empty liposomes in identical buffer conditions (green triangles). (c) Equilibrium unfolding of LeuT in different urea concentration in the presence of 1mM DDM micelles at pH 7.4. Unfolding (black circles) and refolding (white squares) of LeuT in DDM at different concentrations of urea measured by CD intensity at 222 nm. The % folded protein on the Y axis is determined from CD signal intensity at 222 nm; where 100% represents the 222 nm value of fully folded LeuT in DDM and 0% the partly unfolded 8 M urea state (that possesses 65 % of original helical content). The continuous line represents a two-state fit to the unfolding curve, error bars represent standard deviation of at least 5 repeated samples. (d) The free energy of unfolding was determined at different urea concentrations using equation ΔG = -RT ln([unfolded]/[folded]) and data from (*C)*; extrapolation to zero urea gives a ΔG_U^{H2O}=+3.1 ± 0.3 kcal· mol^{-1}. All data shown are a sum of at least 5 repeats each based upon at least 3 separate protein preparations.

Figure 3: Unfolding and refolding of LeuT in liposomes composed of i) 0.8:0.2 DOPC:DOPE and ii) 0.5:0.5 DOPC:DOPE. (a) Far UV circular dichroism of LeuT at a protein lipid ratio of 1:25 (black), unfolded in 8 M Urea and 0.29 mM OG (red) and refolded into 50 mM sodium phosphate pH 7.4 buffer (blue). (b) Transport of ^{14}C Leu into liposomes composed of DOPC:DOPE by LeuT (open circles), 8 M unfolded LeuT (red circles) and refolded LeuT (blue squares). (c) Equilibrium unfolding of LeuT in DOPC/DOPE liposomes at different urea concentrations and 0.29 mM OG at pH 7.6. Unfolding (black circles) and refolding (white squares) were measured by CD intensity at 222 nm. The % folded protein on the Y axis is determined from CD signal intensity at 222 nm; where 100% represents the 222 nm value of fully folded reconstituted LeuT in the relevant lipid composition and 0% the partly unfolded 8 M urea state that still possesses some helical content (between 69 and 73 % of the original). The continuous line represents a two-state fit to the unfolding curve; error bars represent standard deviation of at least 6 repeated samples. (D) The free energy of unfolding was determined at different urea concentrations using equation ΔG = -RT ln([unfolded]/[folded]) and data from (*C)*; extrapolation to zero urea gives ΔG_U^{H2O}=+2.6 ± 0.1kcal· mol^{-1} for 0.8:0.2 DOPC:DOPE and ΔG_U^{H2O}=+ 2.9 ± 0.2 kcal· mol^{-1} for 0.5:0.5 DOPC:DOPE.- All data shown is a sum of at least 6 repeats each based upon at least 3 different protein preparations

Figure 4: Unfolding and refolding of LeuT in liposomes composed of i) 0.8:0.2 DOPC:DOPG and ii) 0.5:0.5 DOPC: DOPG. (a) Far UV circular dichroism of LeuT at a protein lipid ratio of 1:25 (black), unfolded in 8 M Urea and 0.29 mMOG (red) and refoldedblue). (b) Transport of ^{14}C Leu into liposomes composed of DOPC:DOPE by LeuT (open circles) , 8 M unfolded LeuT (red circles) and refolded LeuT (blue squares) (c)Equilibrium unfolding of LeuT in DOPC/DOPG liposomes at different urea concentrations and 0.29 mM OG at pH 7.6. Unfolding (black circles) and refolding (white squares) were measured by CD intensity at 222 nm. The % folded protein on the Y axis is determined from CD signal intensity at 222 nm; where 100% represents the 222 nm value of fully folded reconstituted LeuT in the relevant lipid composition and 0% the partly unfolded 8 M urea state that still possesses some helical content (between 79 and 82 % of the original). The continuous line represents a two-state fit to the unfolding curve, error bars represent standard deviation of at least 6 repeated samples. (D) The free energy of unfolding was determined at different urea concentrations using equation ΔG = -RT ln([unfolded]/[folded]) and data from (*C)*; extrapolation to zero urea gives ΔG_U^{H2O}=+2.5 ± 0.1kcal· mol^{-1} for 0.8:0.2 DOPC:DOPG and ΔG_U^{H2O}=+3.8 ± 0.2 kcal· mol^{-1} for 0.5:0.5 DOPC:DOPG.- All data shown is a sum of at least 6 repeats each based upon at least three different protein preparations.

Figure 5: Thermodynamic stability of LeuT correlates with non bilayer PE or charged PG content. Phospholipid compositions composed of DOPC:DOPG shown as black circles and binary phospholipid compositions DOPC:DOPE shown in white circles. In both cases, the unfolding free energy decreases as the amount of DOPE or DOPG is reduced along the x axis. ΔG^{H2O} values were derived from unfolding curves shown in figure 3,4, S7 and s8 at molar ratios of 0.80:0.20, 0.75:0.25, 0.67:0.33, 0.60:0.40 and 0.50:0.50 of DOPC:DOPG or DOPC:DOPE respectively. Error bars describe the standard error of the fitted ΔG_U^{H2O} values.

Figure 6: Values of calculated ΔG_U^{H2O} values for membrane proteins extrapolated from unfolding curves, the first notable examples have been annotated on the figure; all values are summarised in table S1. Circles indicate a-helix proteins where squares indicate B-barrels. Additionally, colour indicates the membrane mimetic used either detergent (white), bicelles (green) or lipid bilayer (blue). Cross strikethrough indicates that steric trapping was used to generate the ΔG_U^{H2O}. For a-helical proteins; DGK is a trimer but the value obtained was for the monomer (14), KcsA is a tetramer and the value obtained refers to tetramer to monomer transition (66), BR structure is stabilised by a co factor (24), DsbB (74)and GlpG (64) area single domain α-helical protein, GalP (11), LacY (12) and LeuT are multidomain α-helical proteins. For B- barrels; OmpA was the first ΔG_U^{H2O} generated for a protein in a bilayer (54, 55), followed by PagP* measured with an N-terminal histag (78), followed with the release of OmpLA (78), OmpW (78) and PagP (78)

Figure 1

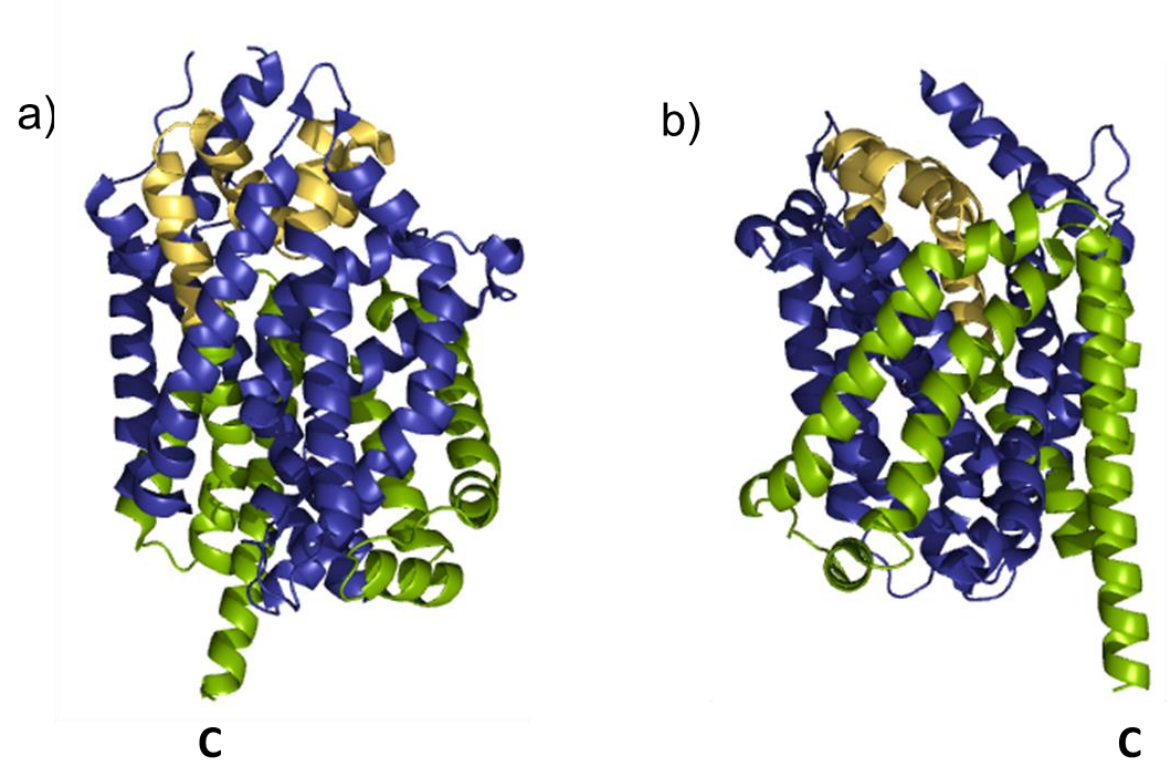

Figure 2

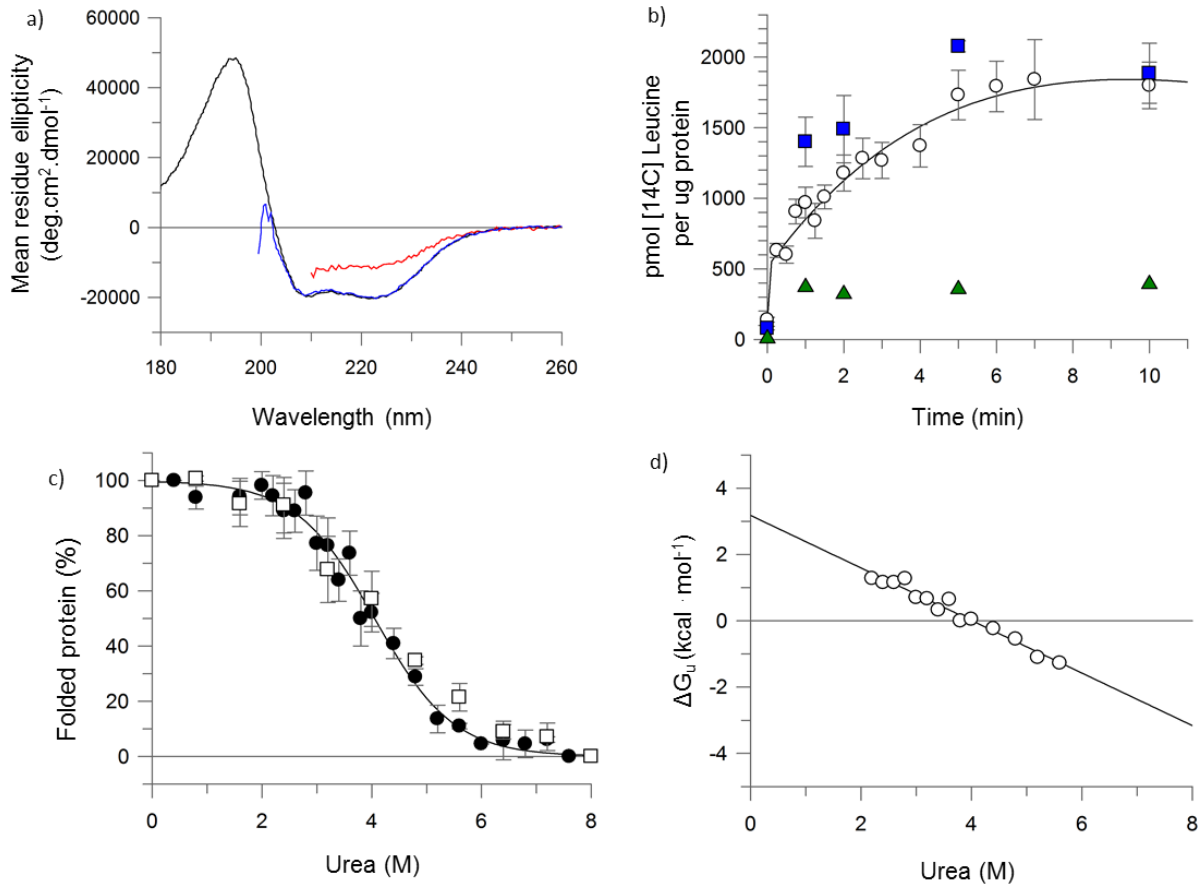
a)
Mean residue ellipticity (deg.cm^2.dmol^{-1})
60000
40000
20000
0
-20000
180
200
220
240
260
Wavelength (nm)
b)
pmol [14C] Leucine per ug protein
2000
1500
1000
500
0
0
2
4
6
8
10
Time (min)
c)
Folded protein (%)
100
80
60
40
20
0
0
2
4
6
8
Urea (M)
d)
ΔG_u (kcal · mol^{-1})
4
2
0
-2
-4
0
2
4
6
8
Urea (M)

Figure 3

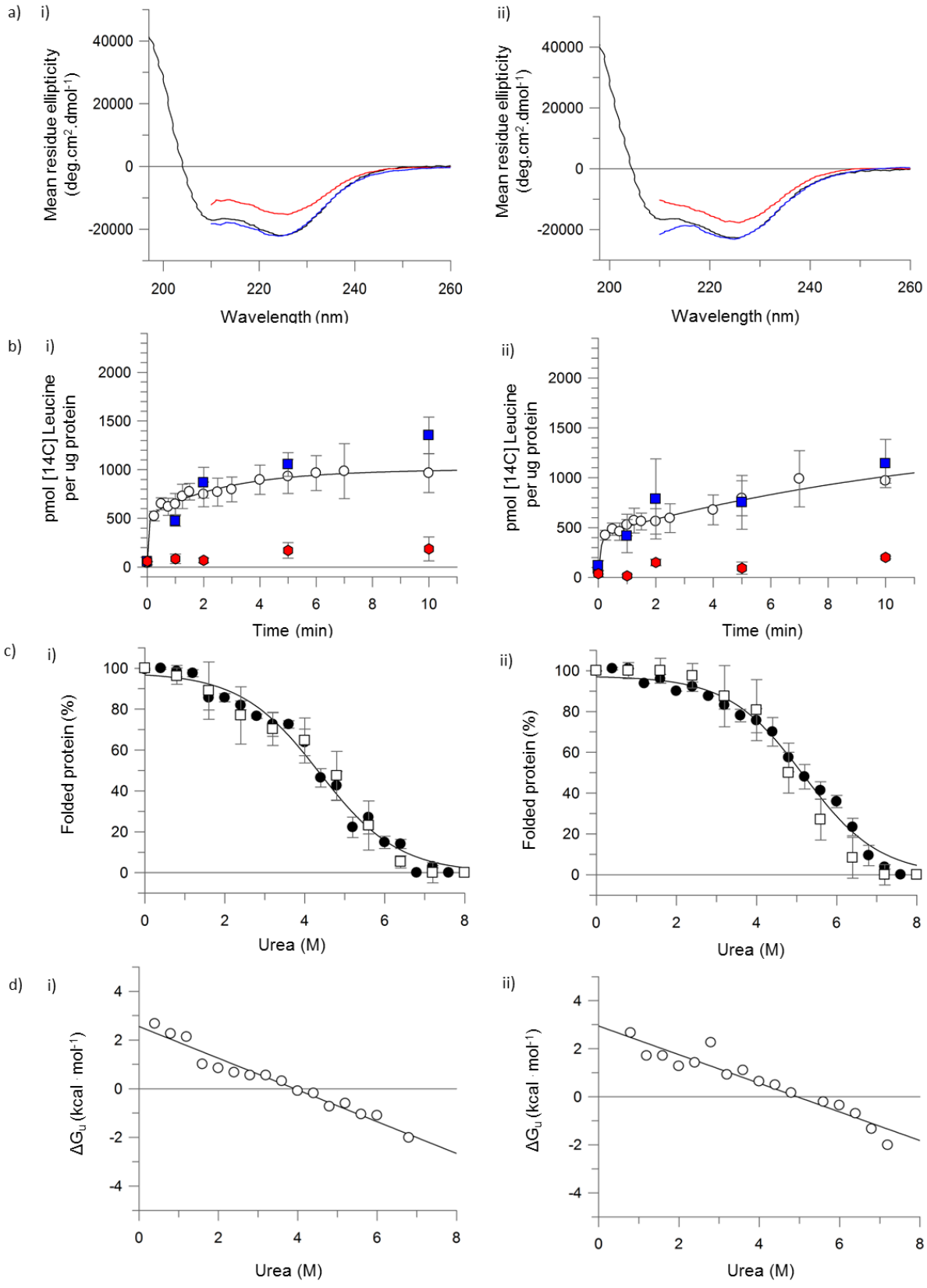
a) i)
Mean residue ellipticity (deg.cm².dmol⁻¹)
40000
20000
0
-20000
200
220
240
260
Wavelength (nm)
ii)
Mean residue ellipticity (deg.cm².dmol⁻¹)
40000
20000
0
-20000
200
220
240
260
Wavelength (nm)
b) i)
pmol [14C] Leucine per ug protein
2000
1500
1000
500
0
0
2
4
6
8
10
Time (min)
ii)
pmol [14C] Leucine per ug protein
2000
1500
1000
500
0
0
2
4
6
8
10
Time (min)
c) i)
Folded protein (%)
100
80
60
40
20
0
0
2
4
6
8
Urea (M)
ii)
Folded protein (%)
100
80
60
40
20
0
0
2
4
6
8
Urea (M)
d) i)
ΔGu (kcal · mol⁻¹)
4
2
0
-2
-4
0
2
4
6
8
Urea (M)
ii)
ΔGu (kcal · mol⁻¹)
4
2
0
-2
-4
0
2
4
6
8
Urea (M)

Figure 4

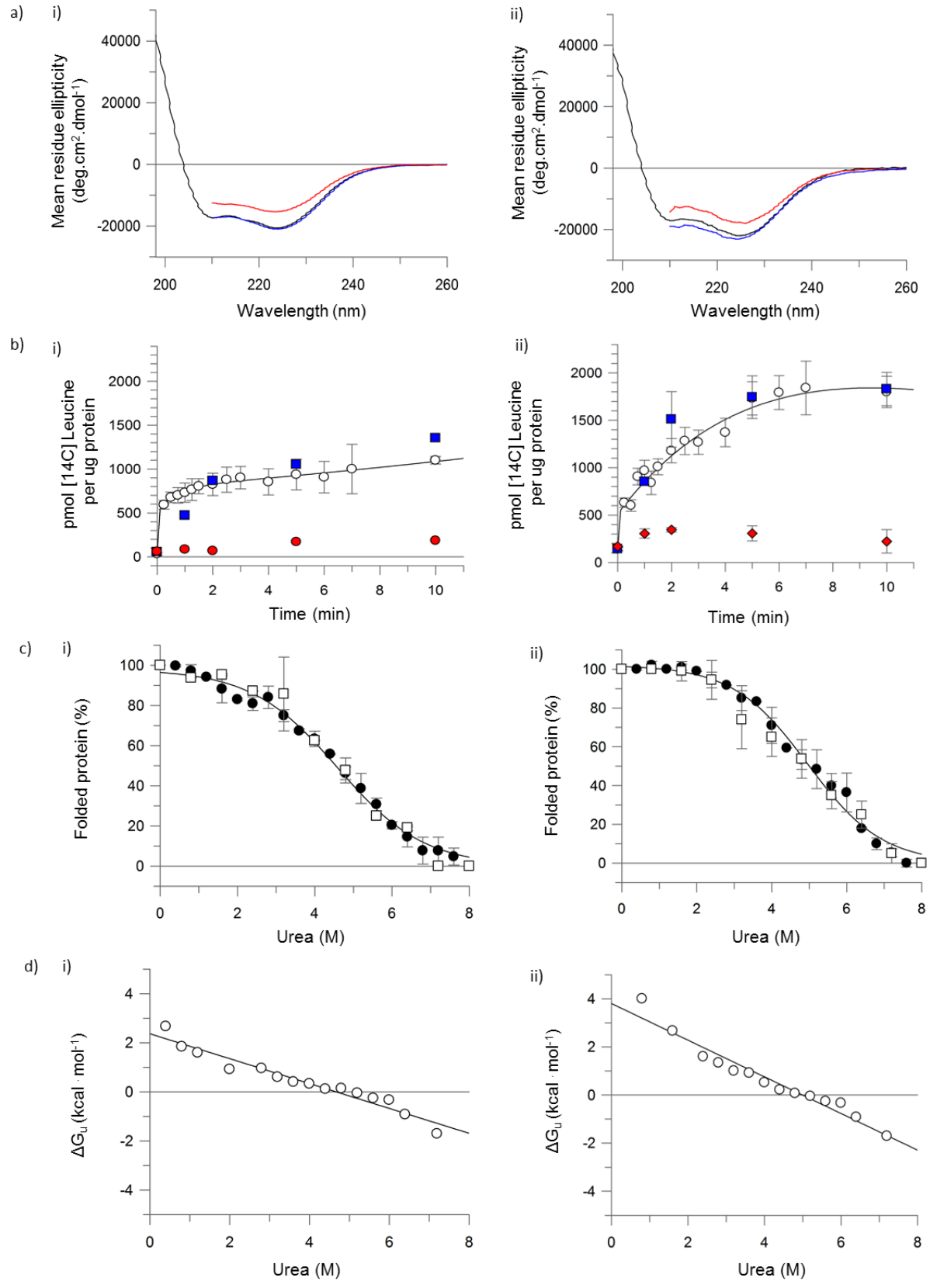
a)
i)
ii)
Mean residue ellipticity (deg.cm².dmol⁻¹)
Wavelength (nm)
b)
pmol [14C] Leucine per ug protein
Time (min)
c)
Folded protein (%)
Urea (M)
d)
ΔGu (kcal · mol⁻¹)
Urea (M)

Figure 5

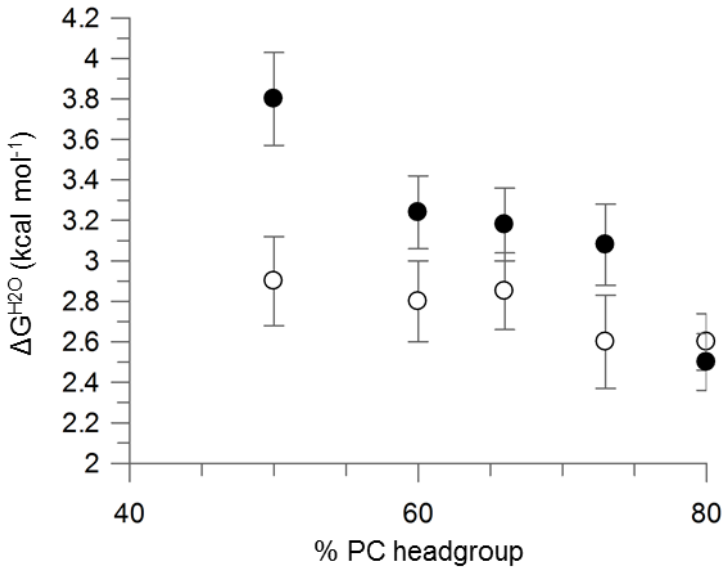

Figure 6

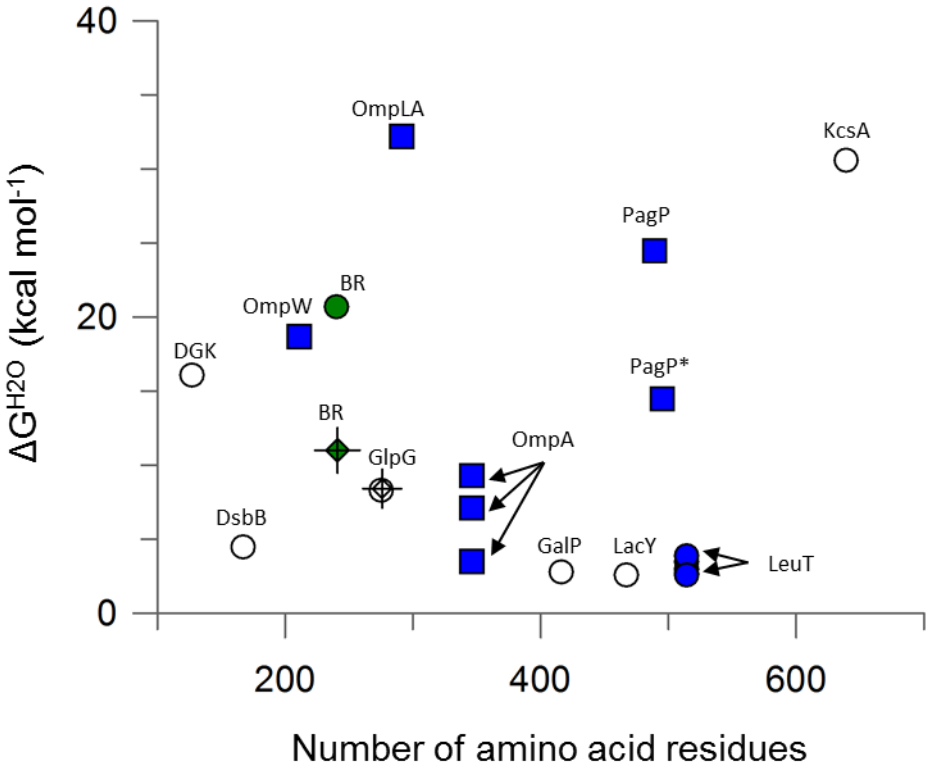

Supplementary Information

SI Results

Crystallographic structure and the polypeptide chain schematic of the entanglement of the knot core compared to the slipknot tail. See fig S1

Native mass spectrometry evidence of monomeric LeuT before use in equilibrium unfolding experiments and before protein reconstitution. See fig S2

Equilibrium unfolding and refolding far UV CD spectra and unfolding curve of LeuT in mixed 1mM DDM-10 mM OG micelles. See fig S3

Comparison of equilibrium folding in liposomes under buffer conditions for folding and transport assay. See fig S4

Comparison of ability of different chaotropes to unfold the protein in the bilayer individually. See fig S5

Evidence of equilibrium folding experiments dependence of the OG concentration in the bilayer in the presence of Urea. See fig S6

Evidence of no change to the lipid phase or liposome particle size upon the addition of either OG or Urea to the bulk. See fig S7 and S8

Evidence of the effect of the presence of 0.29 mM OG in the bilayer during the transport assay and the effect of 0.29 mM OG on bilayer permeability. See fig S9

Equilibrium unfolding and refolding fluorescence spectra monitoring the emission of intrinsic tryptophan fluorescence of reconstituted LeuT in 0.5:0.5 DOPC:DOPE. See fig s10

Equilibrium refolding measured by far UVCD of LeuT in a 0.5:0.5 DOPC:DOPE bilayer when 0.29 mM or 0.04 nM OG is present in the bilayer. See fig S11

Protein concentration independence on loss of secondary structure when unfolded in a bilayer by OG and urea. See fig s12

Equilibrium unfolding curves and the accompanying ΔG_U^{H2O} extrapolations of unfolding of LeuT in different ratios of lipid head group compositions containing DOPC and either DOPG or DOPE. See fig S13 and S14

Equilibrium unfolding and refolding far UV-CD spectra and curves for LeuT folding in 0.5:0.5 DOPE:DOPG accompanied by transport data See fig S15

Summary table of experimental conditions for equilibrium folding measurements in both detergent and lipid bilayers. See table S1

Summary table of ΔG_U^{H2O} values published for integral α-helical and β barrel membrane proteins. See table S2

Supplementary methods and materials

Materials. All reagents were obtained from Sigma-Aldrich or Fisher Scientific UK ltd. Phospholipids were obtained as powder from Avanti polar lipids. Dodecyl maltopyranoside (DDM) was purchased <99.5 % and Octyl-β-Glucoside (OG) from Generon. All reagents purchased were of the highest available grade.

Protein expression and purification. LeuT was expressed in One Shot BL21-AI Chemically competent *E.coli* using Kanamycin resistance containing plasmid pET-28a. Cells were cultured in Terrific broth initially grown at 37 ^{O}C and induced with 0.1 % arabinose and 1 mM IPTG at an OD_{600} of 0.7 AU for 20 hours at 20 ^{O}C. LeuT was expressed in One Shot BL21-AI Chemically competent *E.coli*. Cells were cultured in Terrific broth initially grown at 37 ^{O}C and induced for 20 hours at 20 ^{O}C. .All buffers used in the purification contained 50mM Sodium phosphate (pH 7.4), 10 % (v/v) glycerol, 10 mM β-mercaptoethanol and 1mM DDM, with additional components indicated in brackets. Following growth and induction cells were cracked by a microfluidiser (Constant systems) and the membranes were harvested by centrifugation at 100,000 x g at 4^{O}C for 30 minutes (Beckman Coulter Optima L-80 XP ultracentrifuge, rotor Ti-45). The harvested membranes were resuspended at 50 % w/v in solubilisation buffer (200 mM NaCl, 20 mM imidazole, 40 mM DDM and EDTA free protease inhibitor cocktail tablet (Roche Applied Science) at 4^{O}C for 2 hours. The solubilised membranes were then spun at 100,000 x g at 4^{O}C for 30 minutes where the supernatant was retained for purification. Column purification was carried out using an Akta Pure system (GE healthcare). The supernatant was injected onto a 1 ml HisTrap HP Ni^{2+} IMAC column (GE Healthcare) pre-equilibrated in 10 column volumes of binding buffer (25 mM imidazole). 25 column volumes of washing buffer (75 mM imidazole) was applied to the column after loading to wash unbound contaminating protein. The column was then washed with 4 column volumes of elution buffer (500 mM imidazole). The protein was then injected directly onto a prep grade gel filtration column packed with superdex 200 resin to remove both the imidazole and large aggregates. Purified protein was collected and concentrated using a 100,000 kDa amicon filter.

Circular dichroism Spectroscopy. The same cell containing buffer only was also measured for background subtraction during data analysis. All CD spectra were processed using CDTool (83), Dichroweb (84) and GraFit .

For reversible unfolding in detergent, the final protein concentration of 0.1–0.5 mg ml^{-1} was used in quartz rectangular or circular Suprasil demountable cells of pathlengths 0.1 mm, 0.2 mm or 0.5 mm

(Hellma Analytics). Each sample was scanned two to four times from 260 to 190 nm. Samples containing urea were scanned from 260 to 200 nm due to the high absorbance of urea below 200 nm.

Multiple scans were averaged and the buffer background was subtracted. These processed spectra were then imported in to GraFit for further analysis. The data was converted from mdeg to mean residue ellipticity, based upon protein concentration determined by UV absorbance at 280 nm or by Markwell-Lowry protein concentration assay.

Transport assay. L-Leucine uptake into liposomes was initiated by diluting liposomes loaded with buffer I (50 mM Potassium phosphate (pH 7.4), 250mM Potassium Chloride) with 20 fold excess of buffer II (50 mM Potassium phosphate (pH 7.4), 250mM Sodium Chloride, supplemented with 100 nM ^{14}C Leucine) at 25^{O}C. Transport of the reconstituted wild type protein was maintained for 15, 30, 45, 60, 75, 90, 120, 150, 180, 240, 300, 360 and 600 seconds, whereas for reconstituted LeuT that had undergone unfolding and refolding transport was maintained for 60, 120, 300 and 600 seconds, the transport was stopped by diluting each assay tenfold with ice cold buffer I. This was followed by filtration through 0.22 μM Nitrocellulose filters (Millipore, Watford, UK), the filters were then washed twice with 5 ml of ice cold buffer I. Filters were then placed in vials with ultima gold MV (Perkin Elmer) scintillation fluid and radioactivity was measured in a TRI-CARB 1600TR liquid scintillation counter.

Protein Reconstitution. Detergent saturation was performed by adding octyl glucoside to 100 nm liposomes to a final concentration of 1.2% wt⁄vol and mixed for 20 min. For spectroscopy experiments LeuT was added at a 25:1 ratio by weight, whereas for the transport assay LeuT was added at a ratio of 100:1 and incubated for 60 min. Excess detergent was removed by detergent removal spin columns (Pierce life sciences) and liposomes recovered by centrifugation at 3,400x*g* and resuspended in buffer to 10 mgmL^{-1}.

Intrinsic tryptophan fluorescence. LeuT was reconstituted unfolded and refolded in the manner described in the previous sections. LeuT was reconstituted into liposomes composed of 0.5:0.5 DOPC:DOPE and the intrinsic tryptophan fluorescence measured by excitation 298 nm with the emission spectra collected between 310 and 450 nm. The protein was unfolded and refolded at the same ratios as stated for far UV CD with the protein concentration limited at 0.01 mgml^{-1} to limit detector saturation

Dynamic light scattering. The hydrodynamic radius (R_h) of the liposomes was characterised by dynamic light scattering (DLS). DLS experiments were performed using a Mastersizer S diffraction particle sizer (Malvern Instruments) with a 5003 multi-digital correlator. The light source was a He-Ne laser linearly polarized, with λ = 633 nm, and scattering angle θ = 173°. The lipid solution was continually sonicated until the results of the DLS showed a particle size of a normal distribution around 100 nm by volume derived from the sample's correlation function.

Native mass spectrometry. LeuT was buffer exchanged into MS buffer (0.025 % (w/v) DDM, 200 mM ammonium acetate, pH 8.0, and 5 mM Imidazole) using a centrifugal buffer exchange device (Micro Bio-Spin 6, Bio-Rad). A Synapt G2-Si mass spectrometer (Waters) was used. Typical instrument settings were 1.5 kV capillary voltage, source temperature of 25 °C, argon for trap collision gas, and $1.3e^{-2}$ mbar for trap collision gas pressure. 200 V trap collision voltage, 150 V cone voltage, and 50 V source offset was used; these activation settings enable the removal of DDM detergent bound to membrane proteins whilst maintaining non-covalent interactions (87). Mass spectra, with detector efficiency taken into account, was deconvoluted using the UniDec software program (88). Minimal spectral smoothing was applied to the data prior to deconvolution. Peak widths were determined by fitting peaks to a split Gaussian/Lorentzian model using a 165 *m/z* full width at half maximum.

^{31}P Solid state NMR. Samples for 31P-NMR measurements were prepared in 20 mM Tris HCl pH 7.6 and where s recorded on a Bruker DPX 200 MHz spectrometer at 25°C. A 5-mm broad band probe was used. The ^{1}H-^{31}P decoupling was carried out during excitation and acquisition. All chemical shifts are quoted in parts per million (ppm) with reference to H_3PO_4 in D2O (0 ppm). All spectra were accumulated from up to 30,000 scans.

Vesicle leakage assay. Lipid films were resuspended with 25 mM of CoroNA (Thermo FIsher) sodium sensitive fluorescent dye with 50 mM Potassium phosphate 125 mM Potassium Chloride pH 7.4 before extrusion to 100 nm. 100nm liposomes were then pelleted at 150,00xg for 60 min at 20^{o}C and resuspended in 50mM Sodium phosphate 125mM Sodium Chloride and left to incubate while monitoring excitation 485 nm, emission 516 nm wavelength. As the dye leaked out from the liposome the fluorescence intensity increased, the experiment was repeated in the presence of 0.29 mM OG to determine leakage of the liposomes in the presence of detergent.

Figure S1. .Comparison of the structural topology comparing the knot core to the untangled region of the protein. (a) Shows the different knot components separated from each other i) the knot core ii) the slipknot tail. (c) shows a schematic of the backbone corresponding to the coloured regions in (b) showing the different levels of entanglement within the protein.

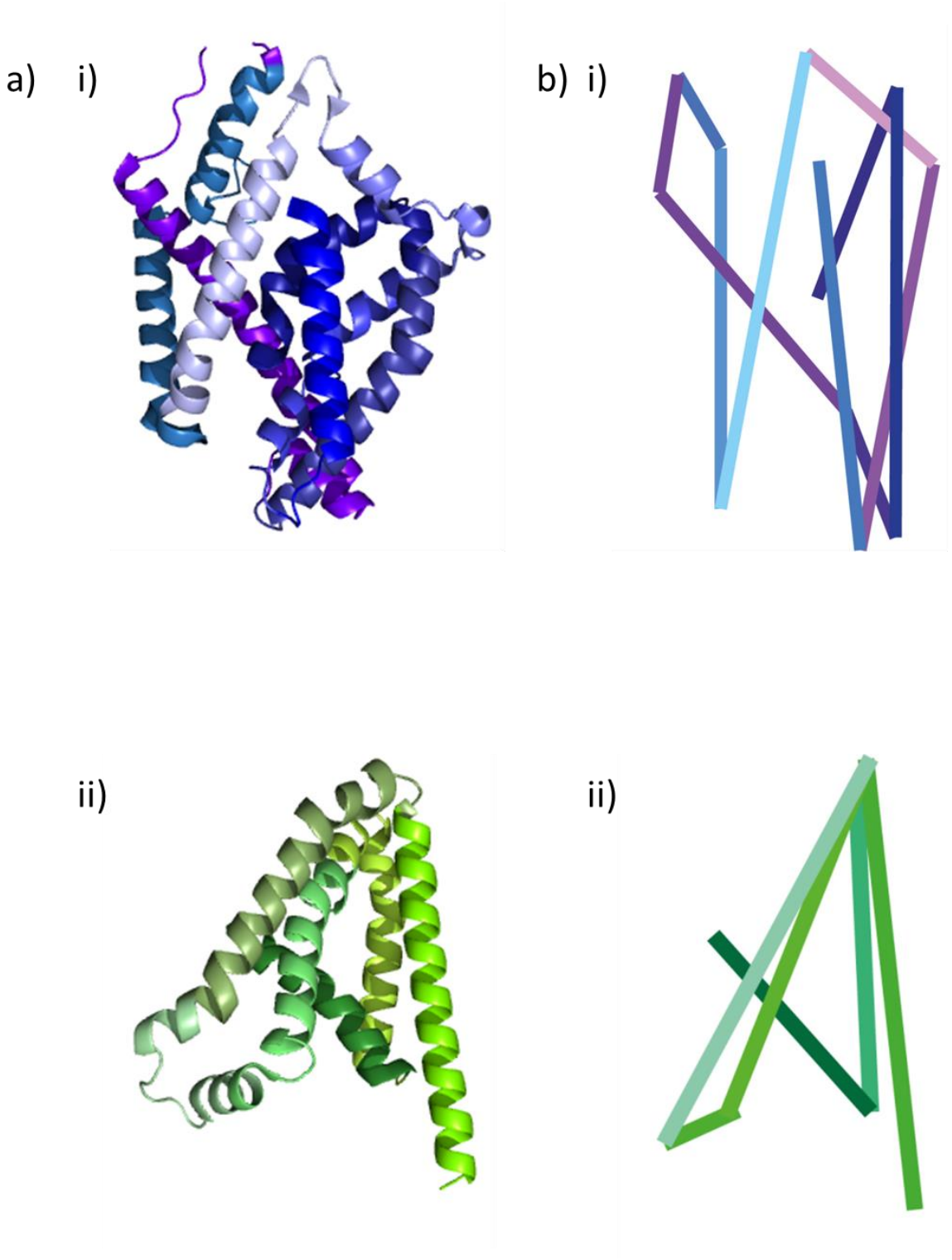

Figure S2. Native mass spectrum data of LeuT , liberated from DDM micelles after 2 hours of solubilisation. The spectrum shows LeuT in a monomeric state but with the additional presence of still bound phospholipid before reconstitution. Repeats were done over different protein preparations of LeuT and consistently showed a mass of around 65 kDa.

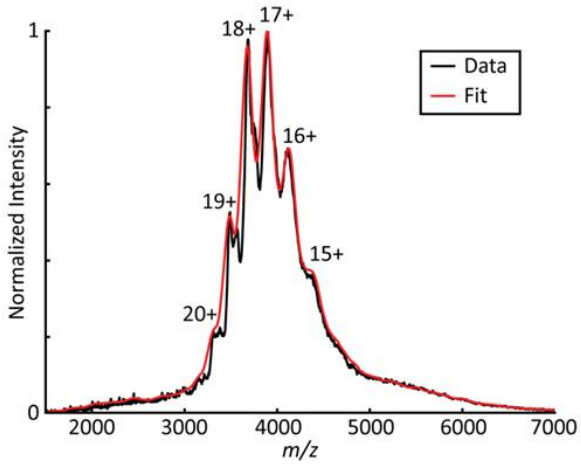
Data
Fit
18+
17+
16+
19+
15+
20+
Normalized Intensity
m/z

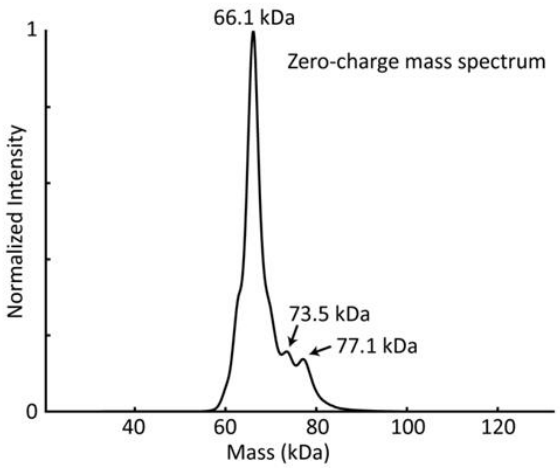
66.1 kDa
Zero-charge mass spectrum
73.5 kDa
77.1 kDa
Normalized Intensity
Mass (kDa)

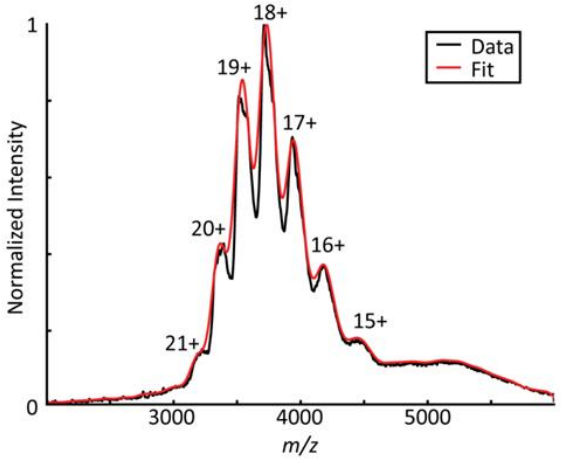
Data
Fit
18+
19+
17+
20+
16+
15+
21+
Normalized Intensity
m/z

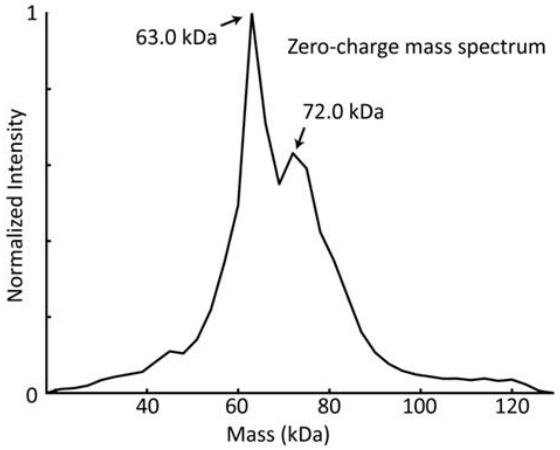
63.0 kDa
Zero-charge mass spectrum
72.0 kDa
Normalized Intensity
Mass (kDa)

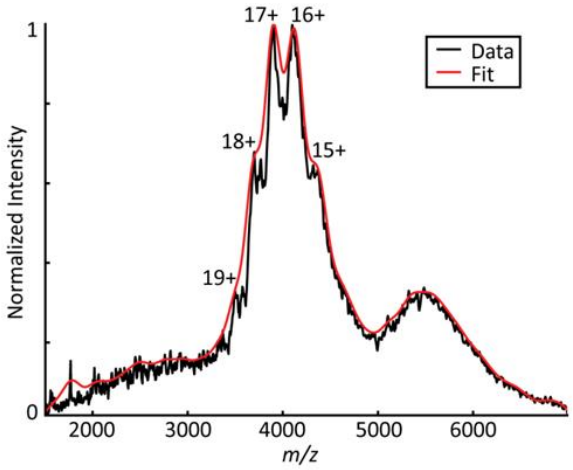
Data
Fit
17+
16+
18+
15+
19+
Normalized Intensity
m/z

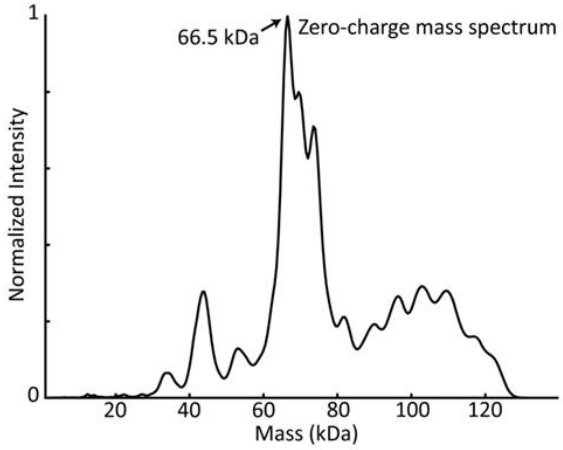
66.5 kDa
Zero-charge mass spectrum
Normalized Intensity
Mass (kDa)

Figure S3. Equilibrium unfolding of LeuT in mixed OG DDM micelles. (a) Far UV CD spectra of LeuT in mixed 10 mM OG/ 1mM DDM micelles (black) unfolded in urea (red) and refolded into mixed 10mM OG/ 1mM DDM micelles. LeuT loses around 35 % of its total secondary structure upon unfolding. (b) Equilibrium unfolding of LeuT at different urea concentrations; unfolding for mixed OG/DDM micelles (white circles) is overlaid with unfolding from figure 2 (c)Data for (b) were measured by CD intensity at 222 nm. The % folded protein on the Y axis is determined from CD signal intensity at 222 nm; where 100% represents the 222 nm value of fully folded reconstituted LeuT and 0% the partly unfolded 8 M urea state that still possesses helical content (90 % of the original structure). The continuous line represents a two-state fit to the unfolding curveThe addition of OG to DDM micelles does not affect the amount of secondary structure loss, urea denaturation curve nor the free energy of unfolding. The ΔG_U^{H2O} value derived from the two state equation is 3.0 ± 0.3 kcal.mol$^{-1,}$ which is consistent with the value of 3.2 ± 0.3 kcal.mol^{-1} in DDM in the absence of OG.

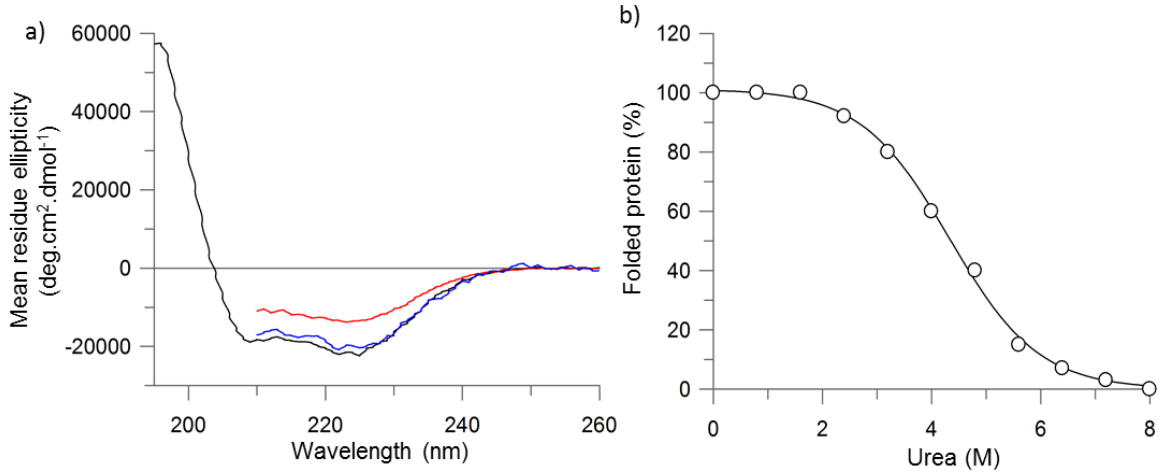

Figure S4. Comparative unfolding of LeuT in 1:1 DOPC:DOPG liposomes in buffer systems. Both potassium and sodium phosphate were used during the transport assay, verification was necessary to show that the buffer system had an influence in unfolding LeuT in the bilayer and no artifacts were bought about by the presence of the counterion. A) Far-UV CD spectra of reconstituted LeuT (black) and of unfolded in 0.29 mM OG and 8M Urea reconstituted LeuT (red) in 50 mM Sodium phosphate pH 7.4 buffer. B) Far-UV CD spectra of reconstituted LeuT (black) and of unfolded in 0.29 mM OG and 8M Urea reconstituted LeuT (red) in 50 mM Potassium phosphate pH 7.4 buffer.

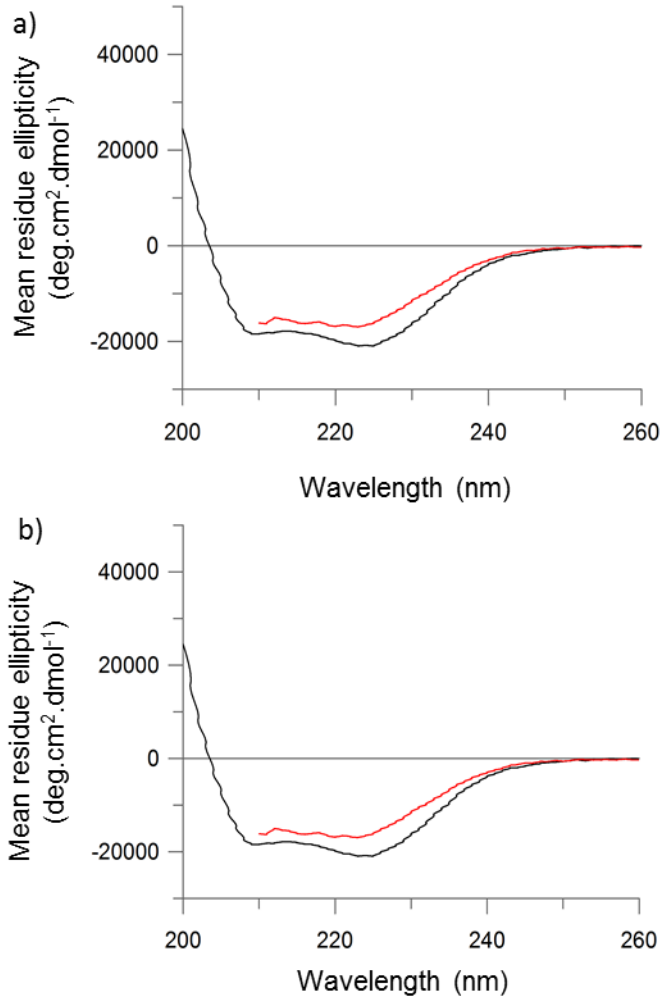

Figure S5. LeuT unfolded easily in the single chaotrope urea when solubilised in detergent, however when this approach was taken when the protein was reconstituted into liposomes there was no evidence of protein unfolding by far UV-CD. Attempted unfolding of LeuT reconstituted into a bilayer composed of 0.5:0.5 DOPC:DOPG measured by far-UV CD. (a) reconstituted LeuT (black) vs 8 M Urea(red) (b) reconstituted LeuT (black) vs 0.29 mM OG (red) and (c) reconstituted LeuT (black) vs 6.4 M Guanidine (red), (d) reconstituted LeuT (black) vs 0.32 mM SDS (red). No unfolding was observed as determined by any reduction in helical structureunder any of these conditions.

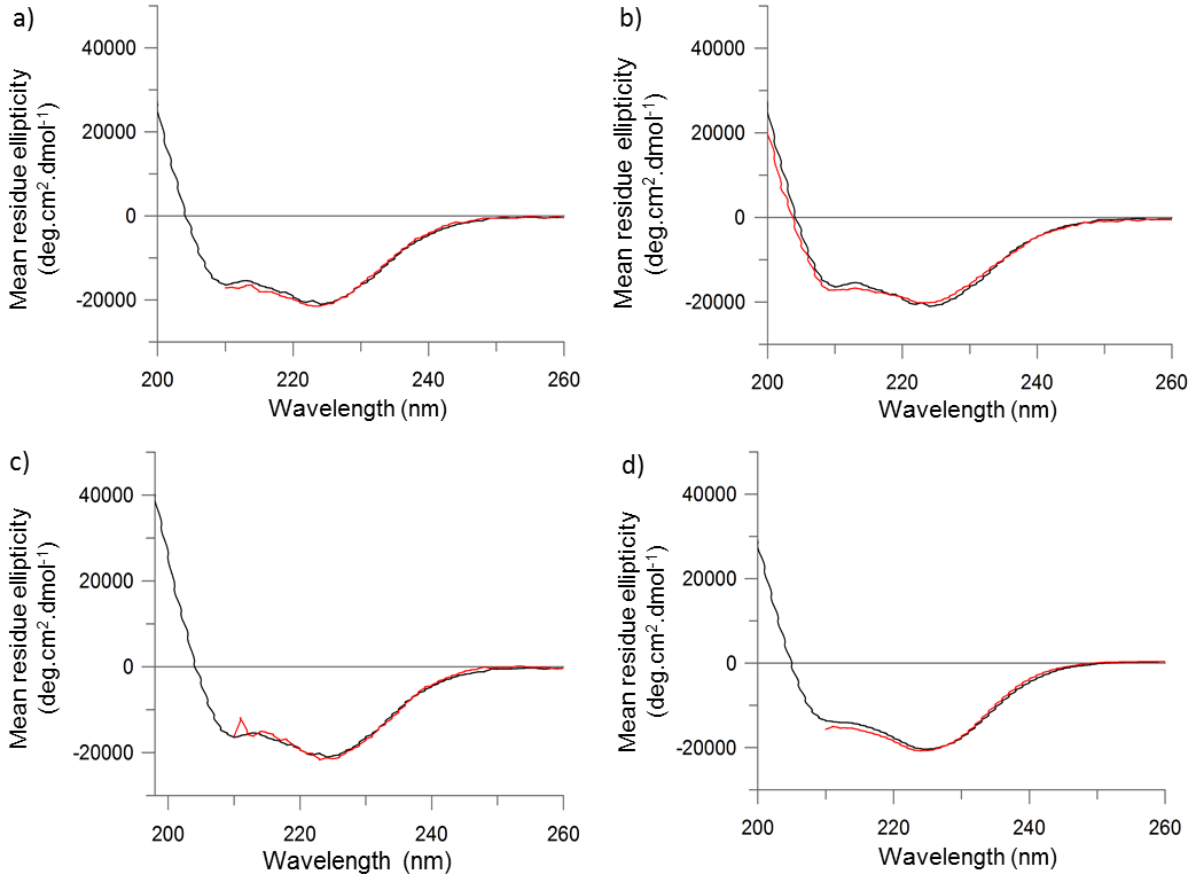

Figure S6. Unfolding of LeuT reconstituted into 0.5:0.5 DOPC:DOPG in the presence of different concentrations of OG. Concentrations of OG were optimised to find the point when the protein would unfold in the presence of 8 M urea and successfully refold after the removal of Urea. A) Far UV CD of reconstituted (black) and unfolded (red) LeuT using 0.60 mM OG and varying concentrations of Urea. B) Unfolding curve of LeuT in 0.60 mM OG and 8 M Urea. C) Far UV CD of reconstituted (black) and unfolded (red) LeuT using 0.17 mM OG and varying concentrations of Urea.

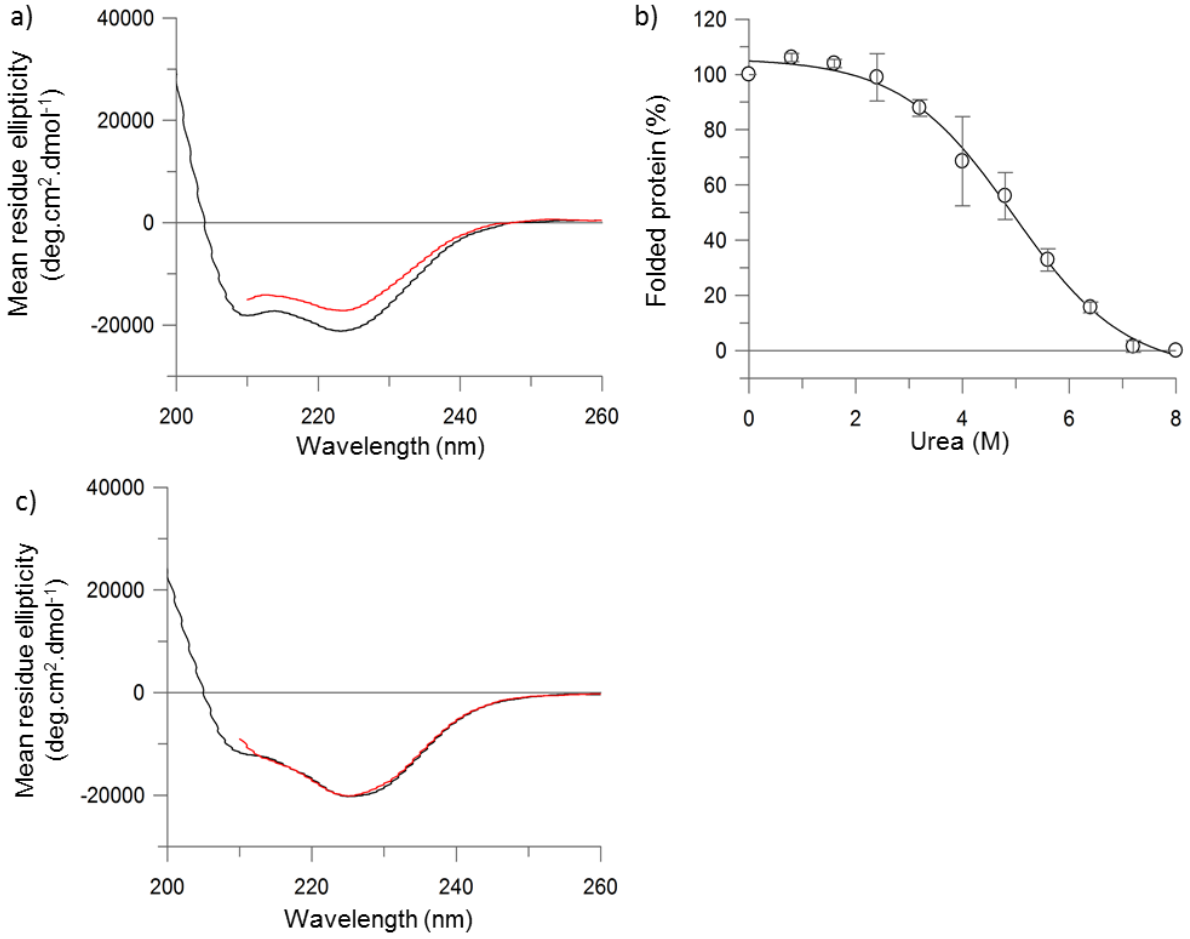

Figure S7. Monitoring effects of protein reconstitution, protein unfolding and protein refolding on the liposome particle size by DLS at 25oC. All size distributions are plotted as functions of intensity. A) 5mM 1:1 DOPC:DOPE liposomes extruded at 100nm giving an Rh of 105 nm by intensity. b) 5mM 1:1 DOPC:DOPE liposomes containing reconstituted LeuT at a protein to lipid ratio of 1:25 giving an Rh of 108 nm by intensity. b. c) 5mM 1:1 DOPC:DOPE liposomes containing reconstituted LeuT at a protein to lipid ratio of 1:25 in the presence of 8M Urea and 0.12 % OG giving an Rh of 110 nm by intensity. b. d) 5mM 1:1 DOPC:DOPE liposomes containing reconstituted LeuT at a protein to lipid ratio of 1:25 after the removal of 8M Urea and 0.12 % OG in 50mM Na PO4 giving an Rh of 107 nm by intensity.

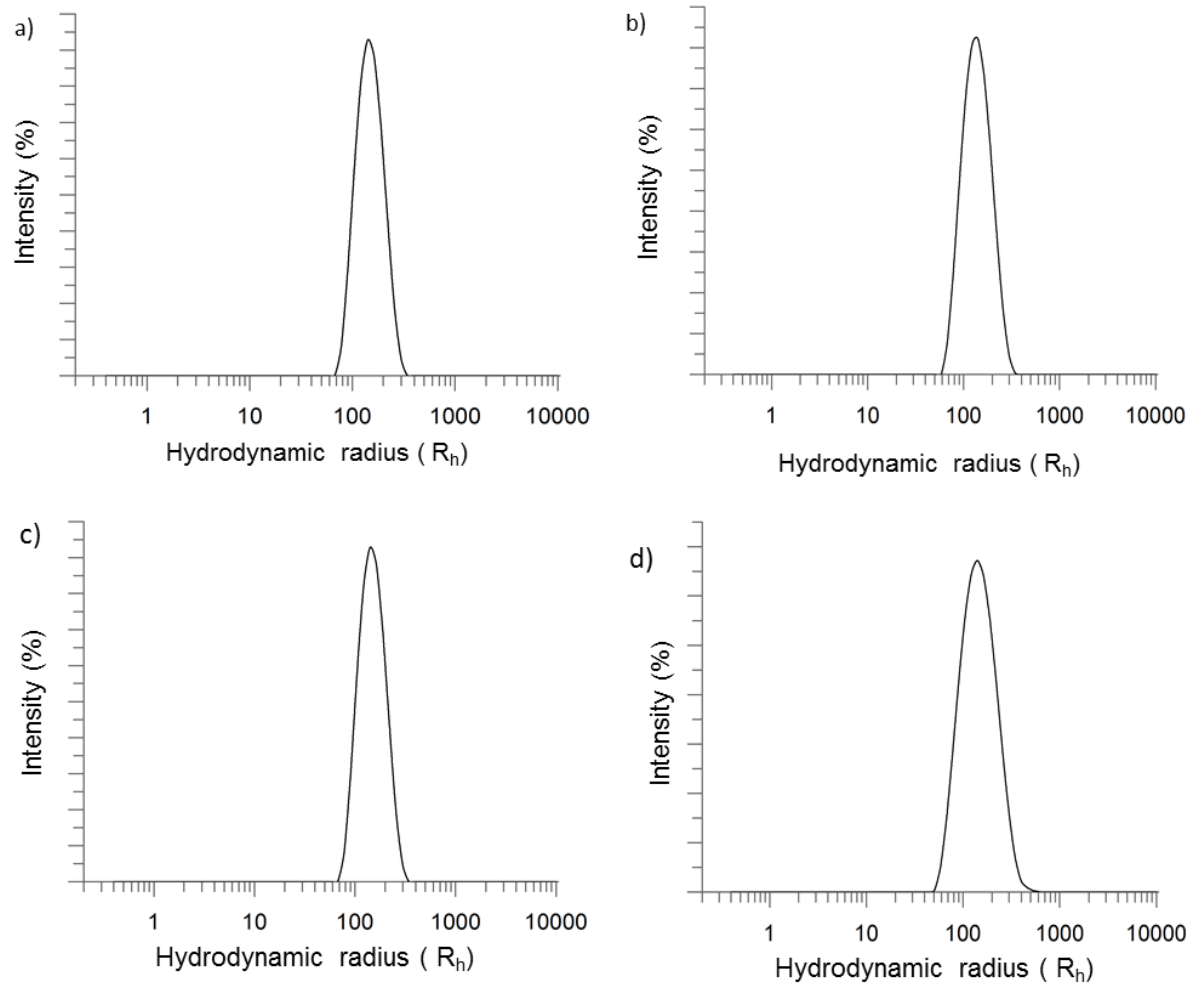

Figure S8. Monitoring effects of the bulk solvent on the phase of the lipid by ^{31}P 50mM Sodium phosphate pH 7.4 (a) and 50mM Sodium phosphate pH 7.4 plus 8M Urea and 0.29 mM OG (b)

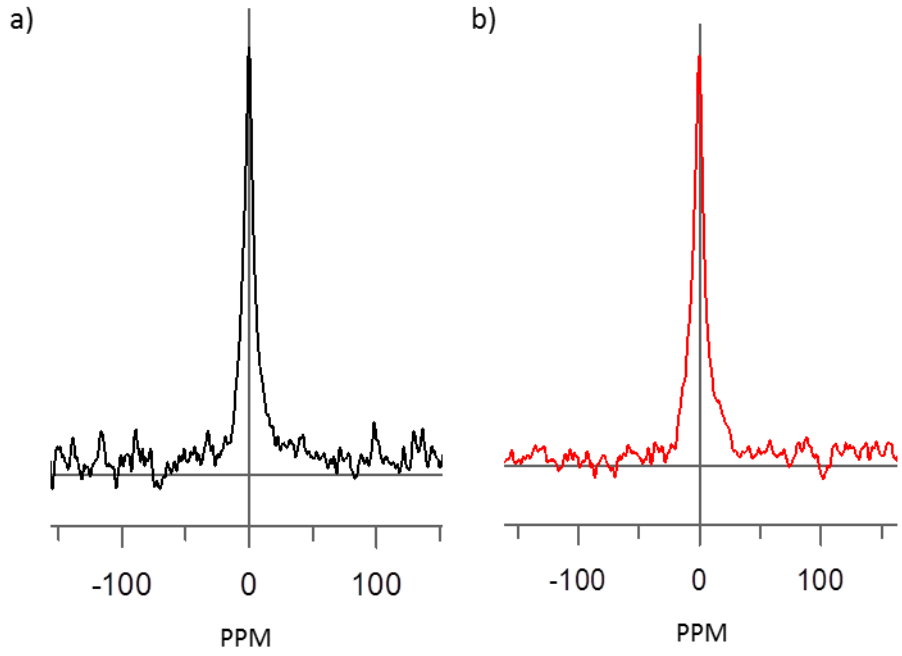

Figure S9. Monitoring the effects of 0.29 mM of OG added to a membrane composed of 0.5:0.5 DOPC:DOPG (a) and the effect of OG on the functionality of reconstituted LeuT (b). (a) LeuT (white circles) displays the same functionality as shown in figure 2, when 0.29 mM OG added to the bilayer no functional transport of LeuT is observed. b) Liposome dye leakage assay showing increased liposome leakage upon addition of OG to the bilayer (red) compared to leakage without any OG present(black). The presence of 0.29 mM OG in the bilayer prevents the formation of a stable electrochemical gradient and prevents transport from being observed.

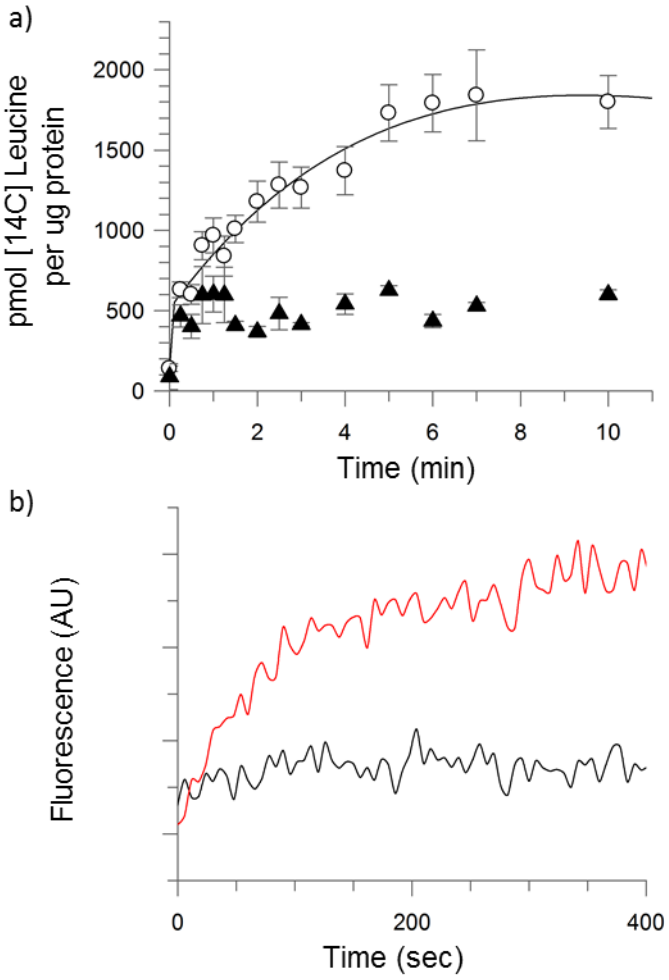

Figure S10. Monitoring the effects of unfolding by 0.29 mM OG and 8 M urea on intrinsic tryptophan fluorescence of LeuT in a membrane composed of 0.5:0.5 DOPC:DOPE. Fluorescence spectroscopy is consistent with a significant change of teritary structure in the presence of 0.29 mM OG and 8M urea (red), which was returned upon the removal of OG and urea (blue). Wildtype LeuT(black) reconstitured into a lipid bilayer has 14 trp residues in its primary structure; so intrinsic trp fluorescence is not an accurate measure of loss of tertiary structure.

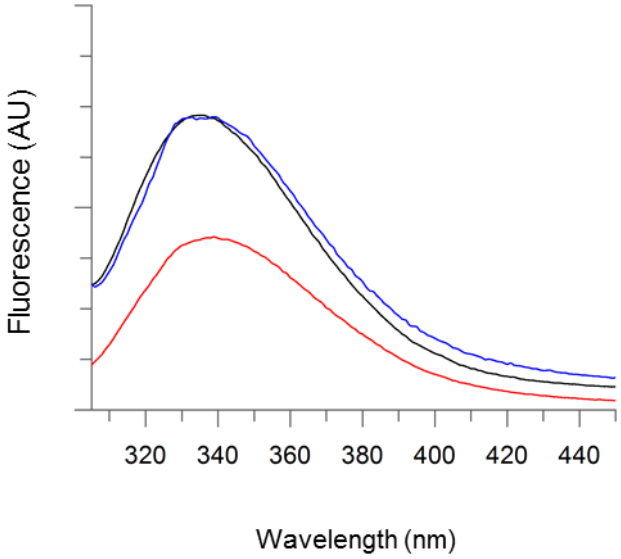

Figure S11. Refolding efficiency of LeuT was independent of the amount of detergent in the bilayer during refolding demonstrated using far UV CD a) Refolding in the presence of 0.29 mM OG in a 0.5:0.5 DOPC:DOPE bilayer, LeuT native reconstituted (black) and refolded protein in the bilayer (blue) and (b) In the presence of 0.04 nm OG in the bilayer: LeuT native reconstituted (black) and refolded protein in the bilayer (blue).

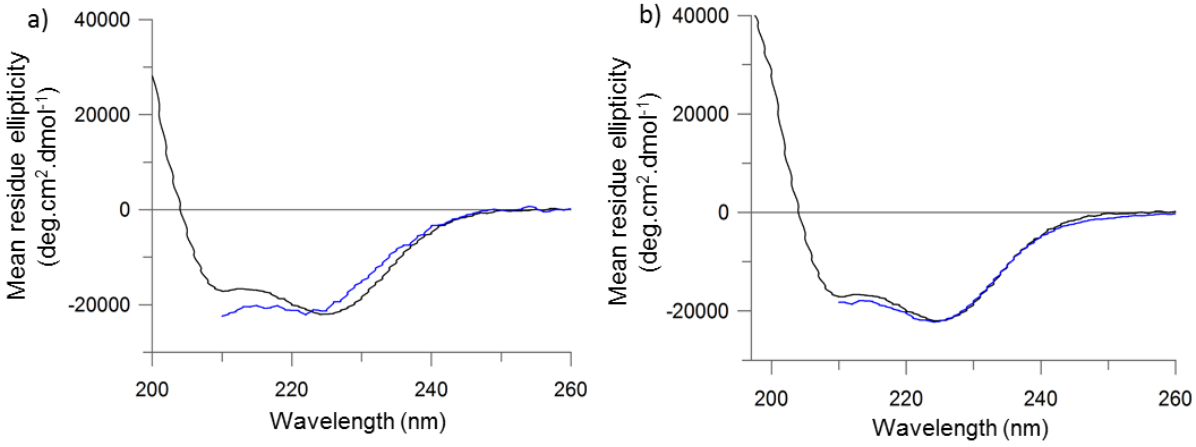

Figure S12. Protein concentration independent unfolding of LeuT reconstituted into 80:20 DOPC:DOPG. Loss of secondary structure was plotted against the Urea concentration used using different prtoein concentrations of 0.025 mg ml^{-1}(blue), and 0.2$mgml^{-1}$ (red) with a comparison against the data presented in figure 3 (white) of around 0.1 $mgml^{-1}$ where the concentration varied dependent on the lipid composition and between different reconstitutions (concentration values are shown in table S1).

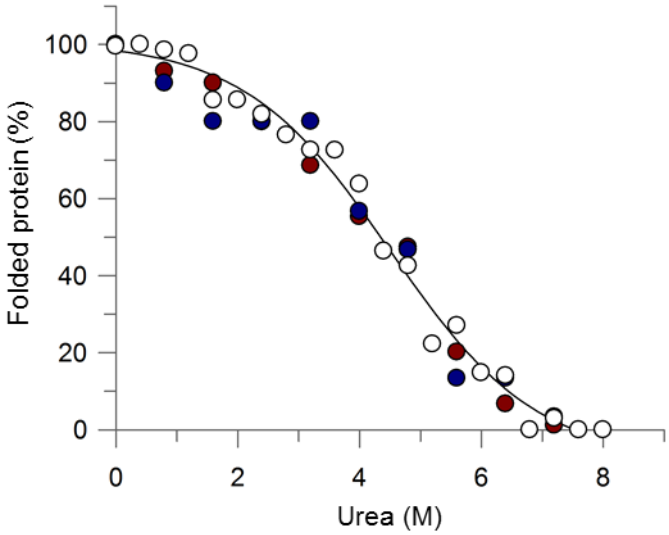

Figure S13. Equilibrium unfolding of reconstituted LeuT in different urea concentrations and 0.12 % OG at pH 7.6 at molar ratios of 0.75:0.25 (a), 0.67:0.33 (b), and 0.60:0.40 (c) DOPC:DOPE. (i) Unfolding (white circles), was measured by CD intensity at 222 nm. The % folded protein on the Y axis is determined from CD signal intensity at 222 nm; where 100% represents the 222 nm value of fully folded reconstituted LeuT and 0% the partly unfolded 8 M urea state that still possesses helical content. The continuous line represents a two-state fit to the unfolding curve. (ii) The free energy of unfolding was determined at different urea concentrations using equation ΔG = -RT ln([unfolded]/[folded]) and data from (*i)*; extrapolation to zero urea. All data shown is a sum of at least 2 repeats each based upon at least two biological repeats.

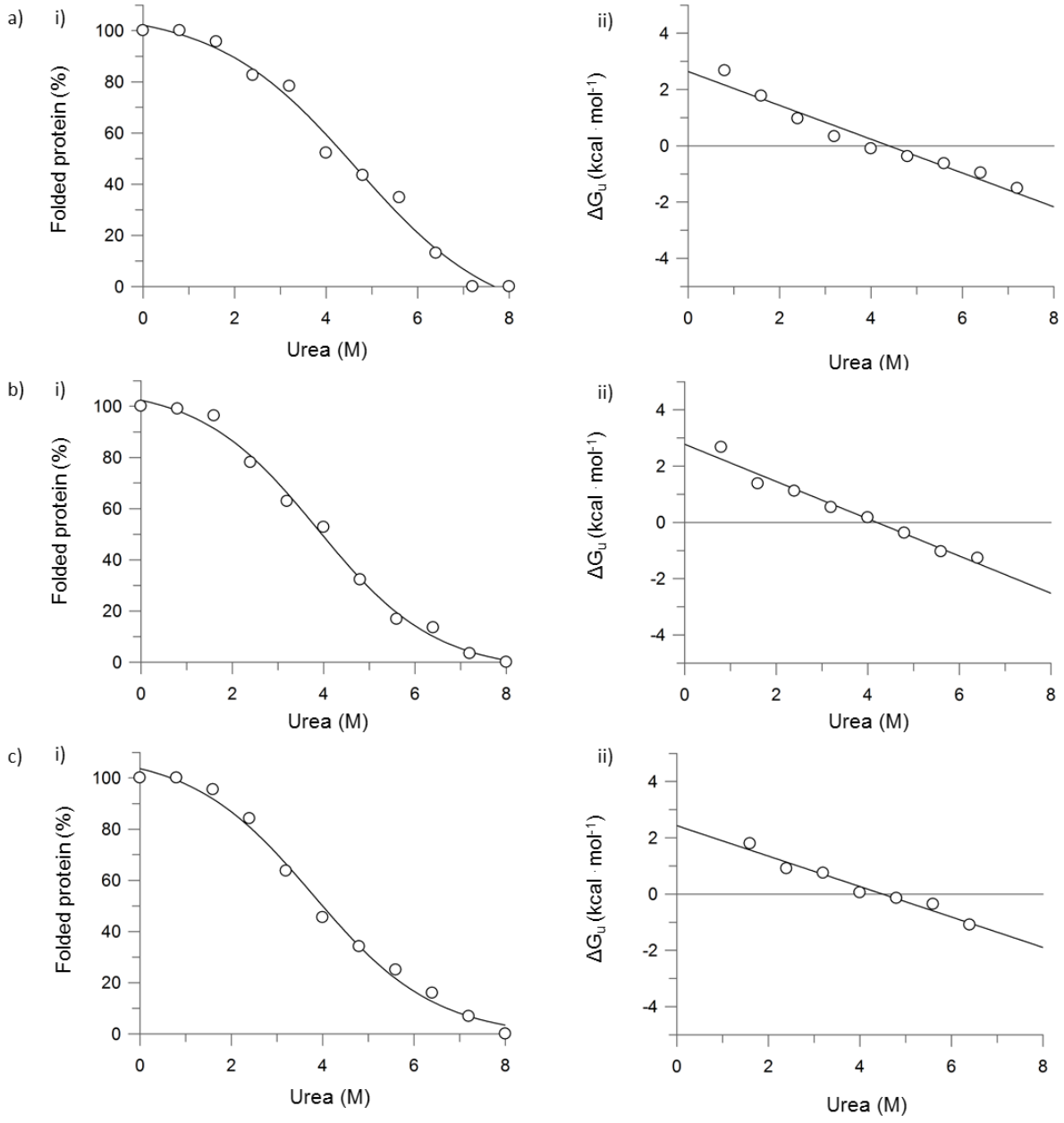

Figure S14. Equilibrium unfolding of reconstituted LeuT in different urea concentrations and 0.12 % OG at pH 7.6 at molar ratios of 0.75:0.25 (a), 0.67:0.33 (b), and 0.60:0.40 (c) DOPC:DOPG. (i) Unfolding (white circles), was measured by CD intensity at 222 nm. The % folded protein on the Y axis is determined from CD signal intensity at 222 nm; where 100% represents the 222 nm value of fully folded reconstituted LeuT and 0% the partly unfolded 8 M urea state that still possesses helical content. The continuous line represents a two-state fit to the unfolding curve. (ii) The free energy of unfolding was determined at different urea concentrations using equation ΔG = -RT ln([unfolded]/[folded]) and data from (*i)*; extrapolation to zero urea. All data shown is a sum of at least 2 repeats each based upon at least two biological repeats.

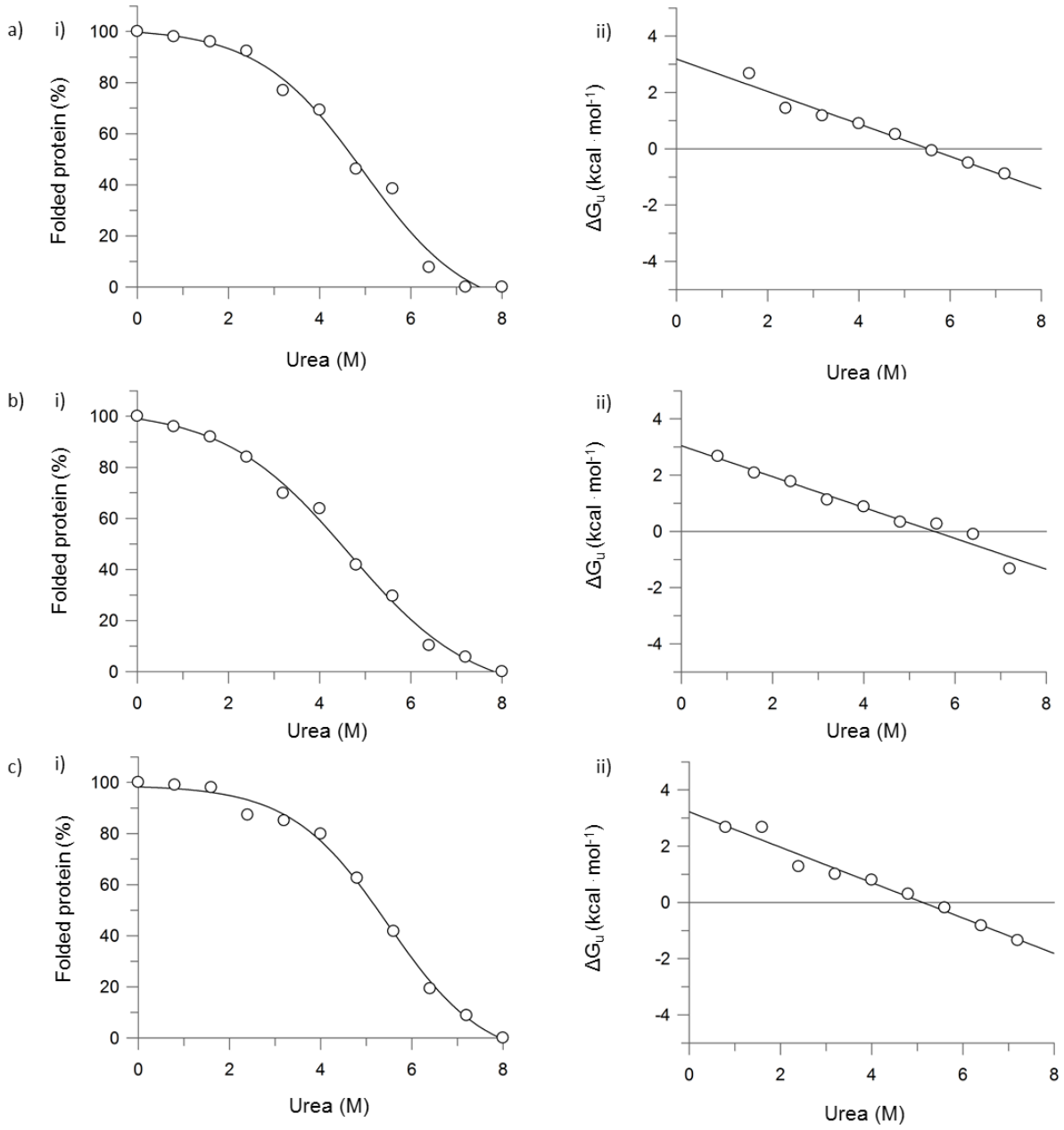

Figure S15. Figure 6: Unfolding and refolding of LeuT from Urea in liposomes composed of 1:1 DOPG:DOPE. (a) Far UV circular dichroism of LeuT (black), unfolded in 8 M Urea and 0.29 mM OG (red) and refolded (blue). (b) Transport of ^{14}C Leu into liposomes composed of 1:1 DOPG:DOPE, LeuT(open circles) , unfolded reconstituted LeuT (red circles) and refolded reconstituted LeuT (blue squares) (c) Equilibrium unfolding of LeuT in different urea concentrations and 0.29 mM OG at pH 7.6. Unfolding (white circles),equilibrium refolding (black squares). Data for (c) were measured by CD intensity at 222 nm. The % folded protein on the Y axis is determined from CD signal intensity at 222 nm; where 100% represents the 222 nm value of fully folded reconstituted LeuT and 0% the partly unfolded 8 M urea state that still possesses helical content (90 % of the original structure). The continuous line represents a linear fit to the unfolding curve. All data shown is a sum of at least 4 repeats each based upon at least 3 different protein preparations.

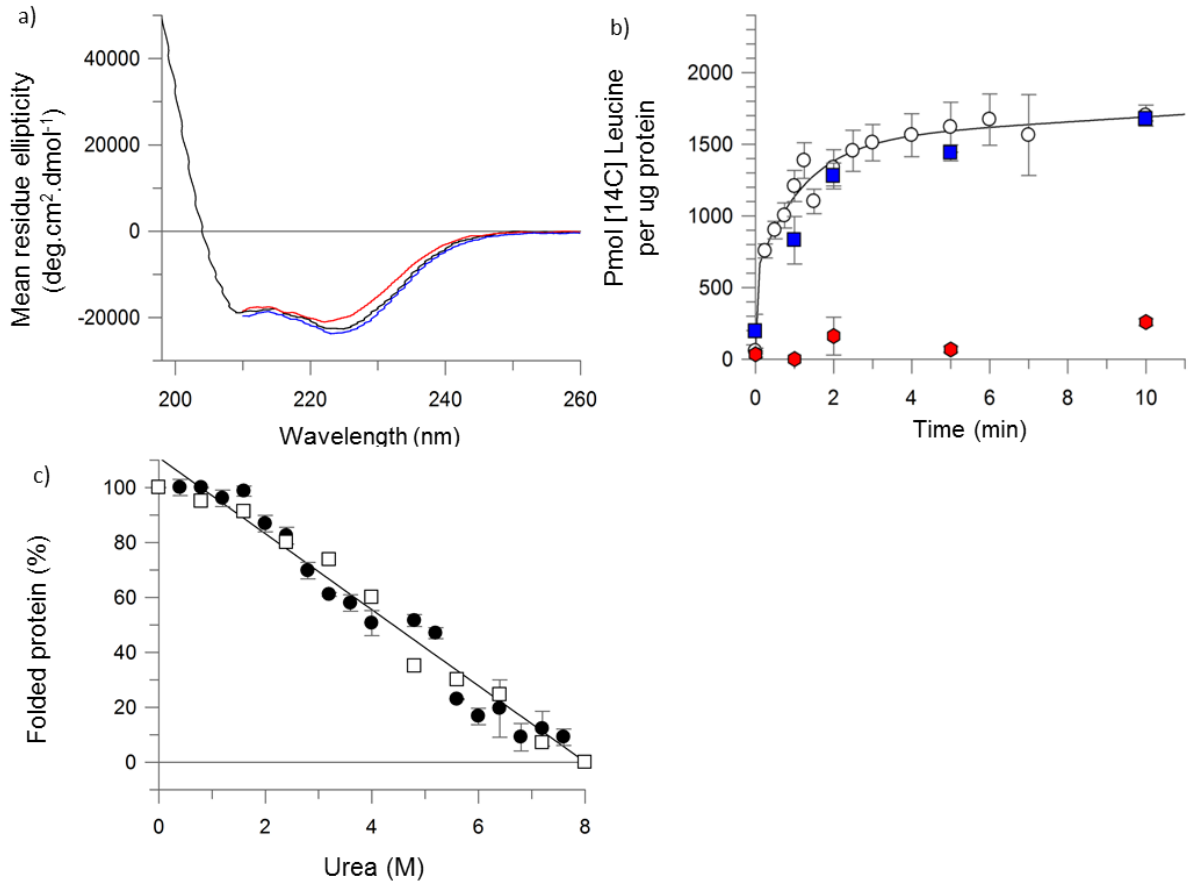

Table S1: Experimental conditions for equilibrium unfolding experiments in both detergent and phospholipid bilayer environments. Mixed phospholipid compositions are shown in molar fraction, detergents in lipid folding experiments were added to bulk urea solutions.

	Protein concentration (mg ml^{-1}) for unfolding	Protein concentration (mg ml^{-1}) for refolding	Phospholipid concentration (mg ml^{-1})	Detergent concentration (mM)	Denaturant
Detergent					
Dodecyl maltopyranoside	0.15 - 0.3	0.015-0.03	N/A	1 DDM	8 M Urea
Lipid composition					
DOPC: DOPE					
0.80:0.20	0.056 - 0.064	0.056 - 0.064	1	0.29 OG	8 M Urea
0.75:0.25					
0.67:0.33					
0.60:0.40					
0.50:0.50					
DOPC:DOPG					
0.80:0.20	0.084 - 0.092	0.084 - 0.092	1	0.29 OG	8 M Urea
0.75:0.25					
0.67:0.33					
0.60:0.40					
0.50:0.50					
DOPE:DOPG					
0.50:0.50	0.084 - 0.092	0.084 - 0.092	1	0.29 OG	8 M Urea

Table S2: Results of equilibrium unfolding experiments showing the starting mean residue elipticity (MRE), the resulting change in MRE, the total amount of secondary structure loss, the midpoint of the two state fit, the resulting ΔG from the linear transformation and accompanying m-value

	222 nm Intensity folded (MRE)	222 nm intensity unfolded in 8 M Urea (MRE)	% reduction in total helicity	Mid point of two state reaction	Δ G free energy (kcal mol^{-1})	m-value free energy vs urea (kcal/mol/M)
Detergent						
DDM	-20000	-13000	35 ± 3	4.1 ± 0.1	3.1 ± 0.3	-0.71 ± 0.06
Lipid composition						
DOPC: DOPE						
0.80:0.20	-20000	-13800	31 ± 2	4.3 ± 0.1	2.6 ± 0.1	-0.65 ± 0.04
0.75:0.25	-20000	-14000	30 ± 2	4.6 ± 0.3	2.6 ± 0.2	-0.60 ± 0.04
0.67:0.33	-20000	-14200	29 ± 3	3.8 ± 0.2	2.8 ± 0.2	-0.66 ± 0.04
0.60:0.40	-20000	-14200	29 ±3	3.7 ± 0.2	2.8 ± 0.2	-0.54 ± 0.04
0.50:0.50	-20000	-14600	27 ±5	5.1 ± 0.1	2.9 ± 0.2	-0.59 ± 0.04
DOPC:DOPG						
0.80:0.20	-20000	-15400	23 ± 3	4.9 ± 0.1	2.5 ± 0.1	-0.52 ± 0.04
0.75:0.25	-20000	-15800	21 ± 2	4.9 ± 0.2	3.1 ± 0.2	-0.57 ± 0.04
0.67:0.33	-20000	-16000	20 ± 2	4.6 ± 0.2	3.2 ± 0.2	-0.54 ± 0.04
0.60:0.40	-20000	-16000	20 ± 2	5.4 ± 0.2	3.2 ± 0.2	-0.62 ± 0.04
0.50:0.50	-20000	-16200	19 ± 4	4.5 ± 0.1	3.8 ± 0.2	-0.76 ± 0.04
DOPE:DOPG						
50:50	-20000	-18000	8 ± 2	N/A	N/A	N/A

Table S3: Previously published ΔG_u^{H2O} values for membrane proteins; values are presented against the number of amino acid residues in the protein in figure 6. Table adapted from (78) to include all the recent advances with α-helical ΔG_u^{H2O} alongside the β-barrel values

Protein	Free energy (kcal.mol^{-1})	Lipid composition and geometry	Denaturant	Reference
α-helical				
DGK	16.0	DM micelle	SDS	(14)
bR	21.6	DMPC / Chaps bicelle		(24)
	11		Steric trap	(71)
KcsA	30.5	DDM micelle	TFE	(66)
DsbB	4.4		SDS	(74)
GlpG	8.2			(64)
			Steric trap	(75)
GalP	2.5		Urea	(11)
LacY	2.7			(12)
β-barrel				
OmpA	3.4	POPC:POPG 92.5:7.5 SUV	Urea	(55)
	7.0	di$C_{18:1}$PC:POPG 92.5:7.5 SUV		(55)
	9.2	di$C_{18:1}$PC:POPG 89.5:10.5		(54)
PagP with N-terminal histag	14.4	DiC_{12}PC LUV		(78)
OmpLA	32.1		GdnCl	(78)
OmpW	18.6			(78)
PagP	24.4			(78)